BEARING CAPACITY OF FOOTINGS ON UNDRAINED SOFT CLAYS

HANMO WANG

2018

A thesis submitted in partial fulfilment of
The requirements for the award of
Master of Engineering (Civil)
Flinders University, Adelaide Australia

Declaration

I certify that this work does not incorporate without acknowledgement any material previously submitted for a degree or diploma in any university: and that to the best of my knowledge and belief it does not contain any material previously published or written by another person except where due reference is made in the text.

Signed on this 15th October of 2018

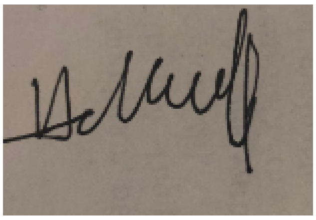

ABSTRACT

The bearing capacity of foundaton is one of most important issue for soil and geotechnical engineering. For foundation safety design, it is necessary to predict stability of footings under saturated or unsaturated soil. The ultimate bearing capacity is the pressure at the base which causes the foundation to failure and a sudden movement. The investigation of undrained bearing capacity of shallow foundation on soft soil is limited in the past and most of data comes from UK's national soil test site, in Bothkennar, Scotland. In recent five years, Australian National Filed Tesing Facility (NFTF) was constructed in Ballina, NSW for site investigation. A series of in situ and laboratory tests were conducted on site in order to investigate the foundation behaviour in terms of load settlement response, soil properties, etc.

During the last few decades, existing methods of estimating short term undrained bearing capacity have been developed by various researchers. Limit equilibrium methods or empirical equations are commonly used for estimating bearing capacity. However, uncertainties such as slope height, distance between footing and excavation wall, soil properties are not considered, which make calculations imprecisely.

In this study, foundation tests data from Ballina is analysed by using empirical bearing capacity theory. The procedures include estimating undrained shear strength, ultimate bearing capacity, effective settlement by using empirical bearing capacity equation and find the load -settlement response for each type of test. A finite element analysis is used to simulate the foundation geometry and load behaviour. The input data for numerical analysis such as Young's modulus, permeability, unit weight of soil, undrained shear strength should be determined from previous foundation tests data. The load settlement response for both hand calculation and numerical analysis are compared in this thesis.

ACKNOWLEDGEMENTS

It is hard to complete this project without the help and support of the people around me. I would like to thank my project supervisor Dr. QinHong Yu. His patience for answering questions, urgent feedback, and kindly personality make me possible to accomplish this project.

I am grateful to my family, my parents for much support and encouragement of my studies.

CONTENTS

Abstract I

Acknowledgements II

1. INTRODUCTION 1

1.1 BEARING CAPACITY OF FOUNDATIONS 1

2. LITERATRURE REVIEW 3

2.1 INTRODUCTION 3

2.2 GENERALIZED BEARING CAPACITY THEORY 3

2.3 REVIEW OF EARLY APPROACH 4

2.3.1 Settlement 9

2.4 PREVIOUS UNDRAINED BEAIRNG CAPACITY INVESTIGATION 12

2.4.1 Upper bound theory analysis for square and rectangular footings 12

2.4.2 Limit element analysis for bearing capacity 12

2.4.3 Finite element analysis for bearing capacity 15

2.5 LITERATURE SUMMARY 16

3. BEARING CAPACITY OF LARGE-SCALE SHALLOW FOUNDATION IN BALLINA 18

3.1 INTRODUCTION 18

3.2 BACKGROUND OF THE SITE 18

3.2.1 Foundation construction and loading blocks 20

3.3 UNDRAINED SHEAR STRNGTH RELATIONSHIP WITH ULTIMATE BEARING CAPACITY 21

3.3.1 Undrained shear strength for CPT 22

3.3.2 Undrained shear strength for SBP test 23

3.4 SOIL STIFFNESS AND ITS LINK TO SETTLEMENTS 23

3.4.1 Vertical settlement 25

3.5 FINITE ELEMENT ANALYSIS (FEA) 25

3.5.1 Material input 26

3.6 PROJECT TIMELINE MANAGEMENT 26

4. BALLINA CASE RESULTS 29

4.1 RESULTS OF UNDRAINED SHEAR STRENGTH 29

4.1.1 Undrained shear strength for CPT 29

4.1.2 Undrained shear strength for TC and TE 30

4.1.3 Undrained shear strength for SBP test 32

4.1.4 Ultimate bearing capacity for each type of test 33

4.2 RESULTS OF SHEAR MODULUS AND SETTLEMENT 34

4.2.1 Shear modulus results for Triaxial Test 34

4.2.2 Shear modulus results for SBPM 37

4.2.3 Results of elastic shear modulus 38

4.2.4 Results of foundation settlement 39

4.2.5 Results of FEA 40

5. ANALYSIS AND DISCUSSION 43

5.1 Undrained shear strength and settlement 35

5.1.1 Load settlement response for empirical and numerical methods 44

5.2 BOUNDARY IMPACY FOR NUMERICAL ANALYSIS 45

5.3 BEARING CAPACITY EQUATIONS FOR UNDRAINED CLAY 46

6. CONCLUSIONS 50

7. REFERENCE 52

LIST OF FIGURES

Figure 1. Bearing capacity failure mechanism. 2
Figure 2. Failure zones in Prandtl analysis (Prandtl, 1921) 5
Figure 3. Bearing capacity factor (Terzaghi and Peck, 1948) 6
Figure 4. Terzaghi's failure zones 7
Figure 5. Meyerhof's failure zone assumption 8
Figure 6. Settlement components(Das et al, 2014) 10
Figure 7. Coefficients of μ_0 and μ_1 for vertical displacement 11
Figure 8. Depth factor for different methods 14
Figure 9. Shape factor for foundation 15
Figure 10.Site location (Science Direct, 2018) 19
Figure 11. Foundation tests, Ballina region in NSW (Science Direct, 2018) 19
Figure 12. Test distribution (Ballina, 2013) 20
Figure 13 Square footing dimensions 21
Figure 14.Beairng capacity factor (Terzaghi and Peck, 1948) 22
Figure 15. Example of undrained shear strength for SBPM 23
Figure 16. Deviatoric stress- strain graph for TC (Doherty, 2018) 24
Figure 17. Soil stiffness graph for Poisson's ratio at 0.5 (Doherty and Deeks, 2003) 25
Figure 18. Elastic perfectly model (Plaxis 2D, 2018) 26
Figure 19. Undrained shear strength profile for CPT 30
Figure 20. Undrained shear strength profile for TC 31
Figure 21. Undrained shear strength for TX 32
Figure 22. Undrained shear strength for SBPM at 2.15 m 32
Figure 23. Undrained shear strength versus depth for SBPM test 33
Figure 24. Shear modulus profile of TX at depth 4.75 m 34
Figure 25. Shear modulus G_{10} profile 35
Figure 26. Shear modulus G_{50} profile 35
Figure 27. Shear modulus G_{MCCtx} profile 36
Figure 28. Pressuremeter data at varies depth 37
Figure 29. Shear modulus for SBPM 38
Figure 30. Load settlement for each soil stiffenss 40
Figure 31. Plan view of FEA model 41

Figure 32. Mesh generating for FEA model ... 41
Figure 33. Total deformation of foundation ... 42
Figure 34. FEA load- settlement graph ... 42
Figure 35. Load- settlement graph for hand caluclation and numerical analysis ... 44
Figure 36. Failure mechanism for g = 0.34 m ... 45
Figure 37. Failure mechanism for g = 0 m ... 46
Figure 38.Impact of the gap to calculate beaing capacity ... 46
Figure 39. Terzaghi's bearing capacity (Geotechnical Engineering Design, 2015) ... 48

LIST OF TABLES

Table 1. Bearing capacity factor and shape factor from different researchers ... 16
Table 2. Project timeline ... 27
Table 3. Undrained shear strength data for TC ... 30
Table 4. Ultimate bearing capacity for each type of test ... 33
Table 5. Soil stiffness profile ... 36
Table 6. Shear modulus for each tyoe of test ... 38
Table 7. Foundation settlements for TX and SBPM ... 39
Table 8. Foundation performance for UU test ... 39
Table 9. Comparison of undrained shear strength and bearing capacity at foundation level ... 43
Table 10. Settlemen for secant shear modulus ... 44
Table 11. Prandtl's equation data ... 47
Table 12. Terzaghi's equation data (1) ... 47
Table 13. Terzaghi's equation data (2) ... 48

1 INTRODUCTION

In the last few decades there have been a lot of studies to investigate the foundations performance in different soil conditions. Both empirical and numerical methods were developed to improve the accuracy of site investigation. The ability to estimate ultimate bearing capacity plays an important role in the foundation design. In the past theories, it has been observed that the bearing capacity is commonly calculated using empirical equations or from design charts which have been produced based on limit equilibrium or upper bound plasticity calculation. Many of the existing methods can't predict the ultimate bearing capacity precisely due to the lack of considering important parameters of bearing capacity theory, such as the distance of the footing from the slope, bearing capacity factors or soil properties. To understand footing behaviours, it is important to analysis load-settlement response from empirical bearing capacity theory and numerical analysis.

In this project, a prediction exercise for bearing capacity of shallow foundations under undrained unconsolidated (UU) condition in soft clays is discussed. The site investigation was conducted in Australian first National Field Testing Facility (NFTF) in Ballina, NSW. The site has 6.5 hectares area, which offers a space to conduct a series of in situ and laboratory tests can be conducted. The site tests include cone penetration tests (CPT), pressuremeter tests, triaxial tests (TX) etc. The testing data was conducted by surveyors and uploaded to the web application- datamap. Students are free to download relevant data from the application for both study and practise target.

In this study, a geotechnical software- Plaxis 2D is used to conduct finite element analysis (FEA) for Ballina Case. The numerical model was simulated based on the soil properties and a range of variables were accounted for including footing size, slope height, soil types, groundwater level, soil properties etc.

The main objectives of this research program are:

- To estimate the undrained bearing capacity of square footings on soft clay, taking account of limit equilibrium theory and Terzaghi's bearing capacity theory

- Determine parameters that influence the ultimate bearing capacity, which include undrained bearing capacity factors, slopes between footing and excavation wall, undrained shear strength
- Find the relationship between undrained shear strength and soil stiffness with its foundation performance
- Investigate the load- settlement response from penetration, pressuremter, vane tests
- Compare the numerical analysis results with previous tests

1.1 BEARING CAPACITY OF FOUNDATIONS

The following discussion includes several definitions to facilitate the understand of later chapters.

Bearing capacity is defined as the capability of the soil to counteract the pressure placed on it. **The ultimate bearing capacity** is the pressure at the base which causes the foundation to failure and a sudden settlement.

Bearing capacity failure mechanism: The failure model of bearing capacity is categorized into three types, which is shown in Figure 1. The first mode of failure is called general shear failure and extends through all three shearing zones. It often occurs for soils within a hard or dense situation. The second mode is local shear failure and involves rupture of the soil only immediately below the footing. It is often associated with a soft and stiffness soil. The third type of failure is punching shear failure and occurs in very loose of soft soils. The process of deformation of the footing involving compression of soil directly below the footing.

Unconsolidated undrained (UU) test is a triaxial compression test that accounts for the load and drainage condition. In this test, the load applied on the sample is quick and the initial specimen is undrained. The undrained shear strength can be obtained from effective shear parameters- cohesion and friction angle. For UU test, friction angle (θ) = 0°, undrained shear strength S_u = deviator stress $(\sigma_1 - \sigma_3)/2$.

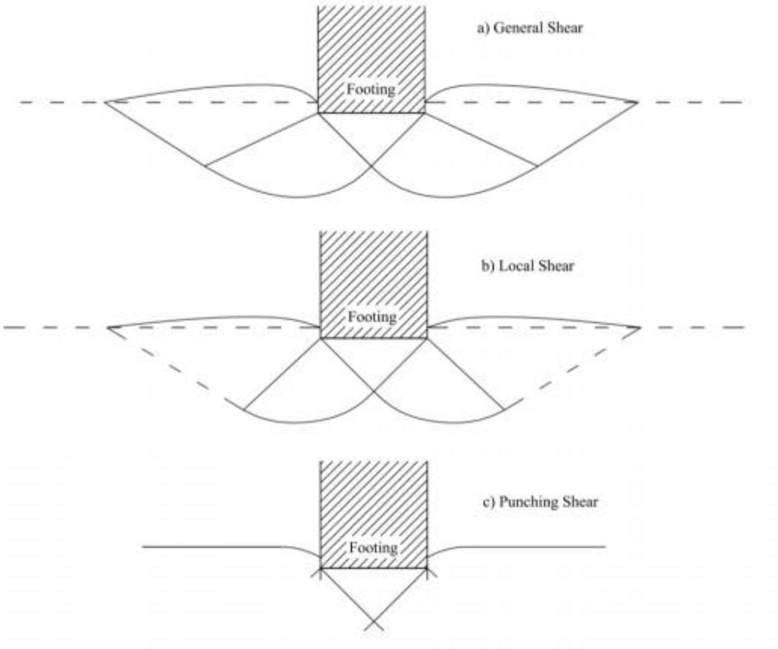

Figure 1. Bearing capacity failure mechanism

2 LITERATURE REVIEW

2.1 INTRODUCTION

Foundation design consists of two important parts, ultimate bearing capacity of footings in soil, and total settlement that the footing mobilizes. Soil properties and footing geometry are two important factors that affect the bearing capacity of footings. Research on bearing capacity has been investigated over one century with either theoretical or experimental methods. While a satisfactory solution is approved only when both methods show the same results.

The previous studies developed multiple complex empirical equations to estimate the undrained bearing capacity. However, the recent advancements in numerical methods for three-dimensional footing analysis such as finite element method can rapidly improve the experimental result.

In this chapter, most current methods of determining bearing capacity are reviewed. A particular emphasis will be placed on discussing uncertainty that affect accuracy of calculating bearing capacity in the last few sections and although some well-known and widely used theory such as Terzaghi's bearing capacity theory, Skempton's bearing capacity factor, and relevant modified theories are discussed. In the past, studies of undrained bearing capacity of foundations on soft clay are limited in the literature. In cases where the soil properties vary with depth, most of past theories cannot be implemented. Likewise, shape and depth factor for foundations could not be estimated accurately. Therefore, it is necessary to compare the recent studies using numerical analysis such as finite element method with empirical solutions to define the accuracy of ultimate bearing capacity.

2.2 GENERALIZED BEARING CAPACITY THEORY

Probably the earliest recorded attempt to solve the problem of bearing capacity of strip foundation was made by Rankine in 1857 (Abedin, 1986). He assumed that failure in the soil is initiated by the formation of two wedges immediately beneath the foundation. While the most known bearing capacity theory was originally developed for cohesionless soils by Pauker (1850) and modified to accommodate cohesive by Bell (1915) and Prandtl (1921). Prandtl developed bilinear failure surface into radial zones through the use of correction factors. The most recent three failure zones are: a triangular active zone, a radial zone and a Rankine passive zone (Terzaghi, et al., 1996). The triangular active zone is the result of active loading forces from the foundation. The radial shear zone was derived assuming a log spiral slip surface in cohesionless soils and is often called the transition zone (Perloff & Baron, 1976). The Rankine passive zone is a result when pressures from loading are transferred to the confining soil via the transition zone (Das, 2011).

The most early well-known bearing capacity theory was developed by Terzaghi (1943) and is applicable for rough continuous foundations. He proposed two-dimensional plane strain model to obtain bearing capacity for strip footing and later, he used three-dimensional mathematical method to account for square and circular foundations. After that, Skempton (1951) found that the depth of foundation impacts the bearing capacity factor, which found the relationship between N_c and ratio of D_f/B. Several different methods exist in the literature to calculate bearing capacity factors. The research presented in this report discussed the Hansen depth factor, Vesic bearing capacity, Meyerhof shape coefficient etc. All these factors influence the result of bearing capacity and should be compared.

2.3 REVIEW OF EARLY APPROACH

2.3.1 Previous studies

Simple plasticity theory was investigated in the early of 20th by Hencky (1924) and Prandtl (1920). In 1921, Prandtl published his study on the penetration of different materials, such as punches, into a weightless soil. He derived a bearing capacity equation with cohesion and bearing capacity factor. In his assumption, the soil weight is not considered.

The bearing capacity given by Prandtl (1921) as

$$q_d = \mathrm{c}N_c \tag{1}$$

$$N_c = \cot\phi[e^{\pi tan\phi}tan^2[\left(45+\frac{\phi}{2}\right)-1] \tag{2}$$

Where: C = cohesion, N= bearing capacity factor

While this assumption is limited by soil type. It only works for cohesive soil such as clay or fined grained soil. While cohesionless soil such as sand or gravel which has zero cohesion, Equation (1.1) gives bearing capacity to zero.

Taylor (1948) reconsidered this formula and figured out this anomaly is due to the assumption that the soil is weightless. Prandtl's equation modified by Taylor is

$$q_d = (\text{c } \cot\phi + \frac{1}{2} YB\sqrt{N_\phi})(\, N_\phi * e^{\pi tan\phi} - 1) \quad (3)$$

Where: Y = unit weight of material

Figure 1 shows the failure zones assumed by Prandtl. It is indicated that zone I is active failure zone which inclined at (45+$\frac{\phi}{2}$) to the horizontal. Zone II is bound by two planes inclined between (45+$\frac{\phi}{2}$) and (45- $\frac{\phi}{2}$) to the horizontal. Zone III is passive zone which inclined at (45-$\frac{\phi}{2}$) to horizontal.

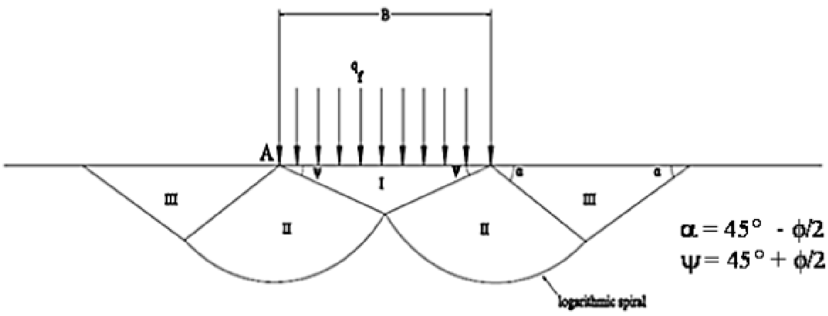

Figure 2. Failure zones in Prandtl analysis (Prandtl, 1921)

Prandtl's theory has limitation on

- The ultimate bearing capacity reduces to zero for cohesionless soil
- The original formula only works for footing resting on surface. Taylor (1948) attempt to optimize Prandtl's formula by considering unit weight of soils.
- The size of footing is not considered in the formula

In 1943, Terzaghi improved Prandtl's plasticity theory to calculate the bearing capacity of strip footings. He assumed the angle that the wedge face forms with the horizontal to be $\emptyset$ rather than the (45+$\emptyset/2$) assumed in Prandtl's theory. He stated that the ultimate bearing capacity of strip footings incorporating three terms of bearing capacity factor:N_c, N_q and N_g, which are related to the friction angle (f'). Hence, he assumed the load works on a rough surface instead of smooth face. Figure 2 shows the three different bearing capacity factors with the angle of internal frictions $\emptyset$. Furthermore, he did not consider the soil property impact to the bearing capacity. He did account for the effects of the soil weight by superimposing an equivalent surcharge load q = YD_f. Although his principle of superposition is not correct, it leads to errors not exceeding 17 to 20 percent for Ø = 30° to 40°. This is equal to zero for Ø = 0

The empirical strip footing formula is

$$q_f = c{*}N_c + q_o{*}N_q + \frac{1}{2}Y{*}B{*}N_g \quad (4)$$

Where $N_c = (N_q - 1)\cot\emptyset'$, $N_q = \frac{e^{2(\frac{3\pi}{4}-\frac{\theta'}{2})\tan\theta'}}{2\cos^2(\frac{\pi}{4}+\frac{\theta'}{2})}$, $N_g = \frac{1}{2}\left(\frac{K_p}{\cos^2\theta'} - 1\right)\tan\theta'$

B = Width of footing, Y = unit weight of soil, D = Depth of footing

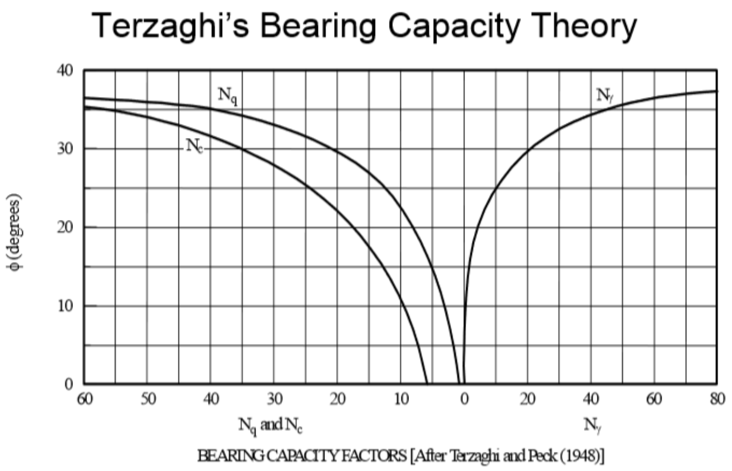

Figure 3. Bearing capacity factor [After Terzaghi and Peck, 1948]

Since the previous formula is worked for strip footing case which uses two- dimensional shape assumption, but in other cases, three-dimensional mathematical view is necessary be used. Therefore, the specific formula which considered shape of footing is developed below

The modified square and circular footing formulas are

$$q_f = 1.3c{*}N_c + 0.4YBN_g + \sigma_q N_q \quad (5)$$

$$q_f = 1.3c{*}N_c + 0.3YBN_g + \sigma_q N_q \quad (6)$$

Figure 4 shows Terzaghi's assumption of failure zones while he derived his equation. These assumptions include:

- The soil mass is homogeneous and isotropic
- The footing has rough base

- The ground surface is horizontal
- The loading is vertical and symmetric
- Zone 1 represents elastic zone which moves downwards during footing failure
- Zone 2 represents radial shear zone bounded between $\emptyset$ and (45-$\frac{\phi}{2}$) to the horizontal
- Zone 3 represents linear shear zone once failure occurs at 45-$\frac{\phi}{2}$ to the horizontal
- The principle of superposition is applicable

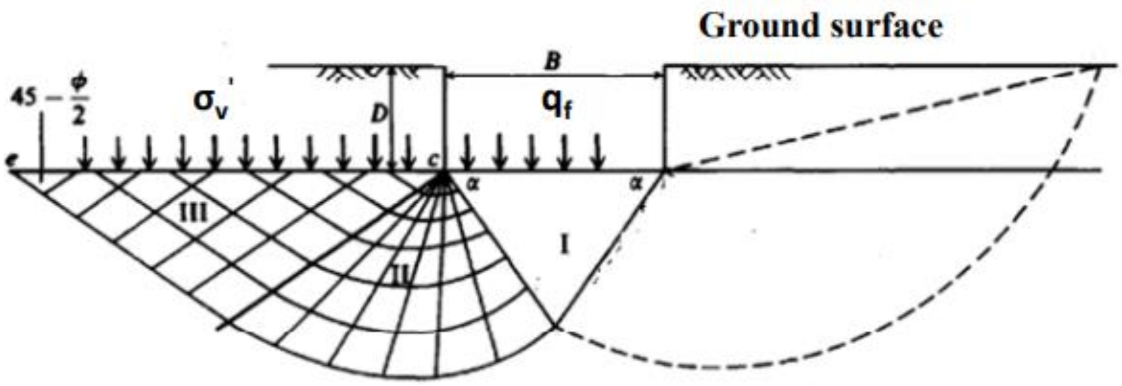

Figure 4. Terzaghi's Failure Zones

Although Terzaghi attempted to optimize Prandtl's bearing capacity theory, his equation was limited by experimentally condition. His theory does not provide the effects of footer depth, load inclination factor or eccentricity, soil compressibility, water table and other factors.

In 1951, Skempton investigated Terzaghi's bearing capacity factor and found that N_c tends to increase with depth in Terzaghi's formula, where N_c increases with increase in D_f/B ratio. He also shows the relationship between ultimate bearing capacities with factor N_c under undrained conditions.

$$q_f = c_u N_c \tag{7}$$

Where c_u = undrained cohesion, q_f = ultimate bearing capacity for saturated cohesive soil under undrained conditions

The relationship between N_c and D_f/B ratio is

For strip footing $N_c = 5(1+0.2\frac{D_f}{B}) \leq 7.5$ (8)

For square and circular footing $N_c = 6(1+0.2\frac{D_f}{B}) \leq 9$ (9)

For rectangular footing N_c = 5(1+0.2$\frac{D_f}{B}$) (1+0.2$\frac{B}{L}$) if $\frac{D_f}{B} \leq 2.5$ (10)

N_c = 7.5(1+0.2$\frac{B}{L}$) if $\frac{D_f}{B} > 2.5$ (11)

Meyerhof (1963) refined Terzaghi's bearing capacity equation and proposed further shape coefficients in his theory. His theory considers the shear strength of soil in the overburden and assumes the boundary of failure zone as a combination of logarithmic spiral failure surface and a free surface.

He introduced shape factor, depth factor and inclination factor in his formula and developed two equations to calculate vertical load bearing capacity and inclined load bearing capacity.

For vertical load:

$$q_f = \text{c}*N_c*s_c*d_c + \sigma_q*N_q*s_q*d_q + 0.5*\text{Y}*\text{B}*N_g*s_g*d_g \quad (12)$$

For Inclined load:

$$q_f = \text{c}*N_c*i_c*d_c + \sigma_q*N_q*i_q*d_q + 0.5*\text{Y}*\text{B}*N_g*i_g*d_g \quad (13)$$

Where: d_c, d_q, d_g = Depth factor, i_c, i_q , i_g = Inclination factor

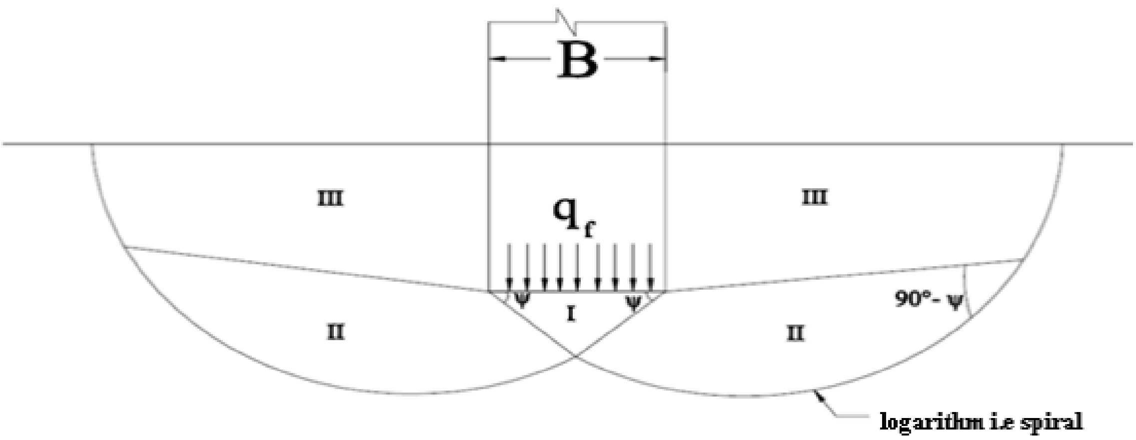

Figure 5. Meyerhof's failure zone assumption

Meyerhof's failure zone assumption is shown in Figure 5. Zone I is elastic zone and Zone II is radial shear zone, as in Terzaghi's assumption. While in Zone 3, the failure zones are assumed above base of footings. Meyerhof's assumption reflects that the shearing resistance of soil above base of footings should be considered.

Brinch Hansen (1970) investigated the previous bearing capacity theory and developed his own formulas for two separate cases of strength parameters; the friction angle $\emptyset$ >0, and $\emptyset$ = 0 (undrained clay). Hansen added ground and base factors in his formula in order to estimate conditions for footing on slope.

For the case: $\emptyset$ >0

$$q_f = cN_cS_cd_ci_cb_cg_c + q_oN_qS_qd_qi_qb_qg_q + 0.5\mathrm{YB}N_yS_yd_yi_yb_yg_y \quad (14)$$

Where q_o = effective overburden pressure, S_c, S_q , S_y = Shape factors, i_c, i_q, i_y = inclination factors, d_c, d_q, d_y = depth factors

For the case: $\emptyset$ =0

$$q_f = (\pi + 2)\, s_u(1+s_{su}+d_{su}-i_{su}-b_{su}-g_{su}) + q_o \quad (15)$$

Where $s_{su} = 0.2\frac{B}{L}$, $d_{su} = 0.4\frac{D}{B}$ for $D \leq B$, $d_{su} = 0.4\,tan^{-1}(\frac{D}{B})$ for $D > B$, $i_{su} = 0.5 - 0.5\sqrt{1-\frac{Q_{tr-B}}{c_aA_f}}$

He suggested the use of Prandtl and Reissner's values for N_c and N_q, and a value of N_y was proposed as:

$$N_y = 1.8\,(N_q - 1)\tan\emptyset \quad (16)$$

Balla (1962) assumed a failure surface, combined with a circular arc and a tangential straight line

2.3.2 Settlement

The settlement of a footing under loading is one of the most important criteria in its structural design. There are many factors which influence the settlement of a foundation. These include the ultimate bearing pressure, the soil layer thickness under the footing and the overburden surcharge.

The total settlement, S_t, that can occur underneath a footing, include three components. The equation is shown as:

$$S_t = S_i + S_c + S_s \tag{17}$$

Where S_i is immediate settlement, S_c is primary settlement, S_s is secondary settlement.

Total soil settlement can be represented by the elastic and consolidation deformation. Figure 6 shows the deformation trend for settlements, which can be identified as three conditions.

Stage 1 is initial compression condition which make deformation rapidly. On the second stage, primary settlement occurs, and water pressure dissipates during the period. Second settlement occurs after the complete dissipation of excess pore water pressure.

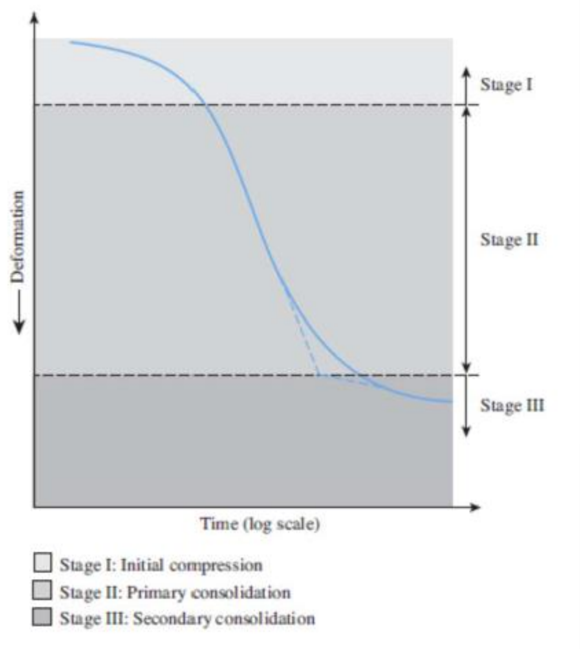

Figure 6. Settlement components (Das et al, 2014)

Total soil settlement can also represent by the sum of elastic settlement and consolidation settlement.

Most of the settlement of foundations on saturated cohesive soil is due to consolidation and associated dissipation of excess pore-water pressure. The vertical settlement of a thin soil layer of finite thickness subjected to uniform loading is:

$$S_i = \mu_0 \mu_1 \frac{qB}{E} \tag{18}$$

Where

μ_0 = Coefficient depending on depth of embedment

μ_1 = Coefficient depending on layer thickness and shape of the loaded area

E = Young's modulus

B = Width of foundation

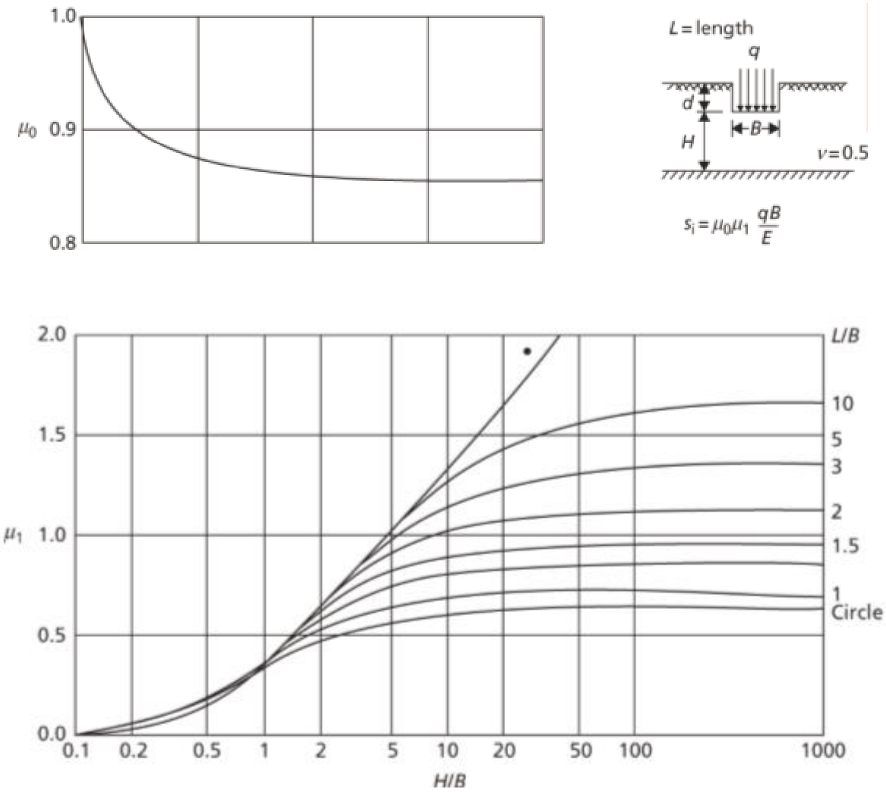

Figure 7. Coefficients of μ_0 and μ_1 for vertical displacement

In a clay layer, primary settlement always takes a couple of months or even years to complete due to the soil properties. Total stress analysis uses the undrained shear strength, s_u, which can be approximated using field tests.

In clays, primary settlement takes year to complete during the project, but varies with other factors such as loading rate or duration of loading. Normal Consolidated clay primary settlement is

$$S_c = \frac{\Delta e}{1+e_o} H_0 \tag{19}$$

Where Δe = Change in void ratio= $C_c \log(\frac{\sigma'_o+\Delta\sigma}{\sigma'_o})$

e_o = Initial void ratio

H_0 = Height of sample

Overconsolidated clay occurs when the present overburden pressure is less than the soil has experienced in the past. The clay properties are mainly dependent on the initial vertical effective stress, σ'_{vo}, and the preconsolidation pressure, σ'_c. The preconsolidation pressure is the maximum previously applied stress. The over consolidation ratio, OCR has a relationship with ratio of initial vertical effective stress and preconsolidation pressure.

$$\text{OCR} = \frac{\sigma'_c}{\sigma'_{vo}} \tag{20}$$

2.4 PREVIOUS UNDRAINED BEARING CAPACITY INVESTIGATION

2.4.1 Upper bound theory analysis for square and rectangular footings

Michalowski (2001) used limit analysis to calculate the bearing capacity of square and rectangular footings and compare with early empirical results. He simplified formula of rate of work dissipation to conduct limit analysis of three-dimensional problems. It was found that internal friction has significantly impact for shape factors. For large internal friction angles (Ψ> 16°) the shape factors are rapidly increasing when the footing aspect ratio drops to 1. He obtained a bearing capacity factor of 6.56 for square footing which is 10% higher than the Meyerhof and de Beer's proposal. The results indicate that Meyerhof and de beer's calculation lack of systematic experimental test, validation of shape factors derived can't be reliably. Therefore, the existing proposals for shape factors are probably conservative. Furthermore, the author suggested that kinematic admissibility is a significant problem for three- dimensional analysis rather than two dimensional problems. Consequently, the estimation of shape factors by upper bound theory are likely overestimated (particularly for large friction angle). Therefore, numerical analysis which do not constraint pattern deformation is recommended to improve solutions for square and rectangular footings.

2.4.2 Limit element analysis for bearing capacity

In the previous review, it can be found that the empirical strip footing formula developed by Terzaghi in 1943 make designers were able to find a foundation framework and develop the former's work. The first exact solution for bearing capacity factor N_c was found by Prandtal (1921) by considering a strip footing with shear strength s_u. After that, a rigid circular footing resting on frictionless soil was investigated by Eason& Shield (1960) by using the Haar-Von Karman hypothesis and slip-line method. While the exact solutions of square and rectangular footings placed at some depth within the soil are not found, instead engineers developed critical factors from theoretical equations to solve these problems. Critical factors such as shape factors and depth factors could not be obtained precisely.

Salagado, et al (2004) investigated the bearing capacities of different shape foundations in clay and used limit element analysis to find the results of critical factors for different foundations. The limit analysis was proved as a tool to solve the bearing capacity problems and stability problems since Hill (1951) and Drucker et al (1951) published their breaking upper and lower plasticity theory. The lower bound theorem emphasizes that the collapse does not happened for a statically admissible stress field. Conversely, upper bound theorem states that collapse is already under way or imminent for an admissible velocity field. These two virtual work equations are represented as:

$$\int_s T_i{}^L v_i \mathrm{dS} + \int_v X_i{}^L v_i \mathrm{dV} = \int_v \sigma_{ij}{}^L \acute{\varepsilon}_{ij} \mathrm{dV} \leq \int_v D\acute{\varepsilon}_{ij} \mathrm{dV} = \int_v \sigma_{ij} \acute{\varepsilon}_{ij} \mathrm{dV} \tag{21}$$

$$\int_s T_i{}^u v_i{}^u \mathrm{dS} + \int_v X_i{}^u v_i{}^u \mathrm{dV} = \int_v \sigma_{ij}{}^u \acute{\varepsilon}_{ij}{}^u \mathrm{dV} = \int_v D\acute{\varepsilon}_{ij}{}^u \mathrm{dV} \geq \int_v \sigma_{ij} \acute{\varepsilon}_{ij}{}^u \mathrm{dV} \tag{22}$$

Where $\sigma_{ij}{}^L$ = statically admissible stress field,

σ_{ij} = stress field

$\acute{\varepsilon}_{ij}$ = strain rate field

v_i = velocity field

$v_i{}^u$ = kinematically admissible velocity field

For strip footings, the bearing capacity is calculated for various depths of embedment. It is clear that the larger bearing capacities at larger aspect ratio due to deeper foundations mobilize massive soil and show that stress rotation is no further important than for shallow foundations. The depth factors can be obtained by dividing the average value of upper and lower bond bearing capacity values. Figure 8 shows the limit analysis results compare with Meyerhof (1951) and Brinch Hansen (1970) relationships for the depth factor. It clearly shows that Meyerhof's depth factors are smaller than expected with the range between 0 to 2.5 D/B ratio and Brinch Hansen factor is unconservative for D/B over 0.5.

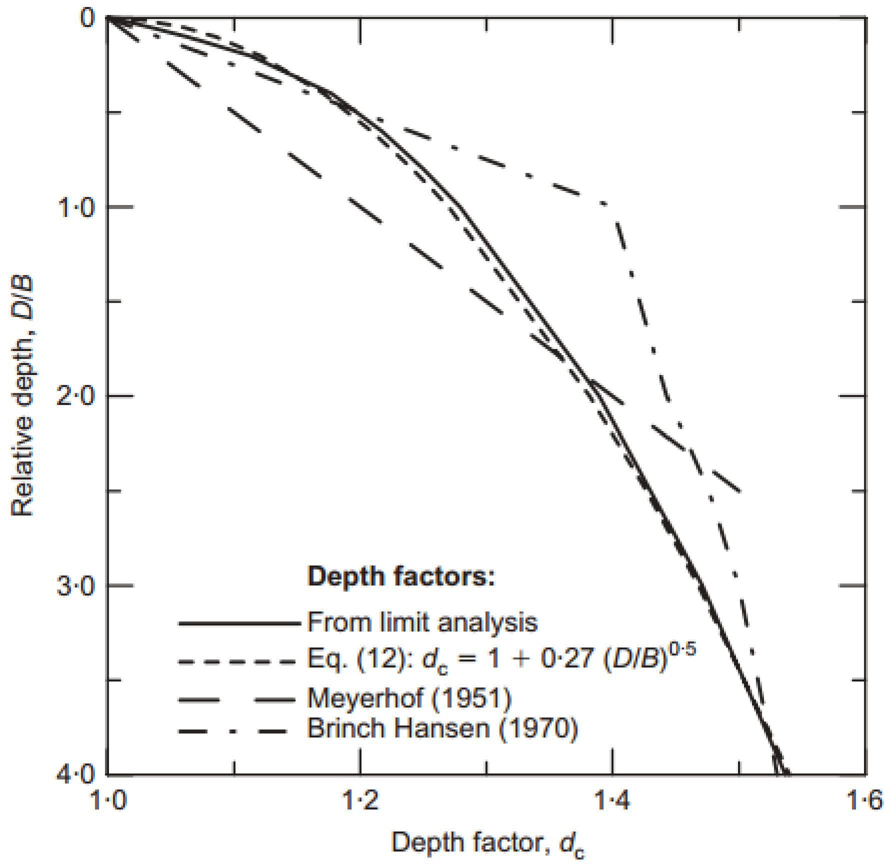

Figure 8. Depth factor for different methods

To obtain the consistent and valuable critical factors, Salagado, et al (2004) investigated the bearing capacity of strip footings relationship with these factors. He derived two equations to express this relationship:

$$s_c = \frac{q^{net}{}_{bL}}{d_c[q^{net}{}_{bL}]_{strip}} \tag{23}$$

$$d_c = 1+0.27\sqrt{\frac{D}{B}} \quad (24)$$

After that, he compared the equation result with Meyerhof (1951) shape factor and found that Meyerhof's shape factor only works for the surface of footing and underestimates the effect of B/L on the limit bearing capacity of deeper footings. Figure 9 shows the shape factor relationship with relative depth of embedment. It reflects the empirical method results of shape factor could be conservative expect very low relative depth.

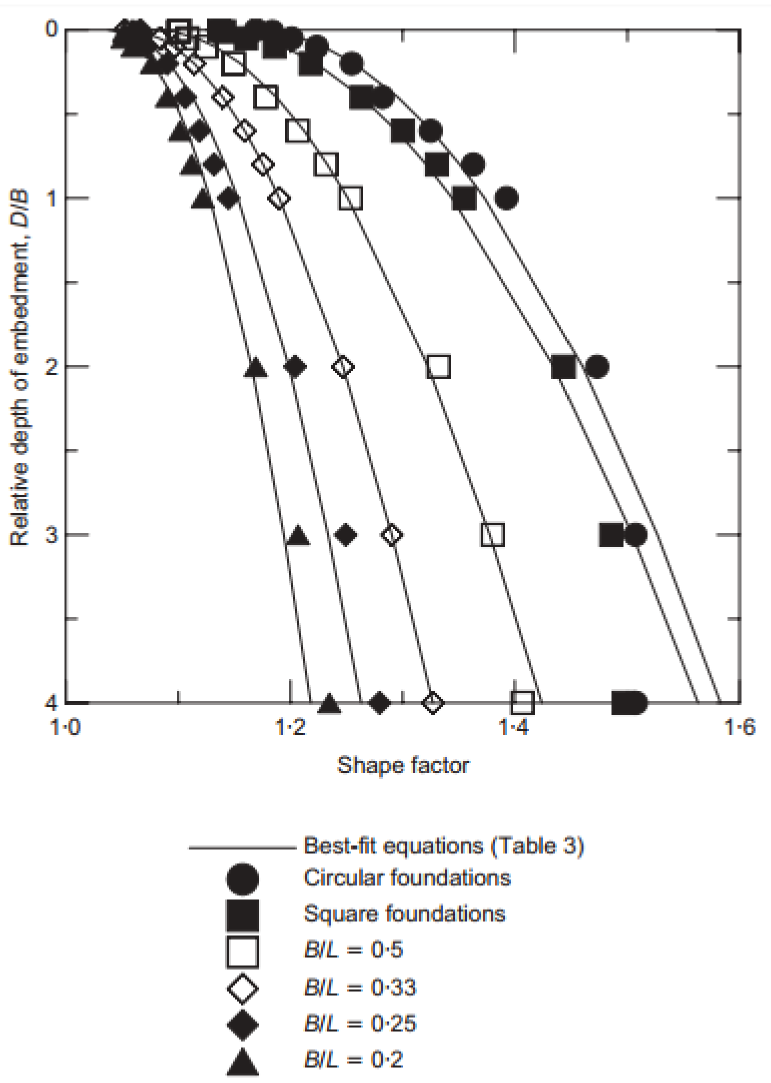

Figure 9. Shape factor for foundations

2.4.3 Finite element analysis for bearing capacity

Susan, et al (2006) investigated the undrained bearing capacity of square and rectangular footings in frictionless and frictional soil with finite-element model to predict the three-dimensional mesh for both footings.

The numerical analysis results are compared with Skempton's bearing capacity theory and a rigorous equation for estimating rough rectangular footings are obtained. During the experiment, some critical factors that impact bearing capacity are calculated. The observations are summarized in the Table 1.

Table 1.

Bearing capacity factor and shape factor from different researchers

Finite element analysis (Susan, 2006)	Skempton's empirical prediction	Salgado's prediction (2004)
Rough square footing	Rough square footing	Rough square footing
N_c = 5.9	N_c = 6.17	N_c = 5.52
s_c = 1.15	s_c = 1.2	s_c = 1.1
Smooth square footing	Smooth square footing	Smooth square footing
N_c = 5.56	N_c = 6.17	
s_c = 1.08	s_c = 1.2	

It was found that Skempton's prediction has same bearing capacity factor and shape factor for both interfaces. The former's prediction likely overestimate the value by 12%.

And upper bound method can over predict up to 10%. This is due to the numerical analysis relates to Kinematic mechanisms at failure. The upper bound theory which using finite element analysis indicates a failure mechanism that has fourfold symmetry. While the optimum mechanisms for a square footing that has only twofold symmetry.

2.5 SUMMARY

The past studies on predicting bearing capacity commonly used empirical equations based on plasticity theory or empirical calculation. Traditional bearing capacity theory does not take important factors that affect bearing capacity into account. In recent studies, researchers start to consider these parameters such as the slope height, distance of the footing from the slope and the soil properties with a combination of numerical analysis such as two-dimensional footing analysis to reduce the uncertainty of bearing capacity.

The literature review has discussed the following points that are relevant to the project.

1. The internal friction angle has significantly impact for shape factors.
2. The shape factor can't be calculated precisely by using upper bond theory (Michalowski, 2001)
3. The value of ultimate bearing capacity relates to the aspect ratio, and stress rotation has less impact to the shallow foundations.
4. It is proved that rough footing has larger bearing capacity than smooth footings.
5. Meyerhof's depth factor is conservative with the D/B ratio, however it only works for surface footings or very shallow footings.
6. Brinch Hansen depth factor is conservative with the D/B ratio over 0.5.
7. Based on finite element analysis, failure mechanisms for square footings exhibit fourfold symmetry.

3 BEARING CAPACITY OF LARGE-SCALE SHALLOW FOUNDATION IN BALLINA

3.1 INTRODUCTION

The investigation of undrained bearing capacity of footings on soft clay is an important issue for foundation design. In this chapter a series of in situ and laboratory tests conducted in Australian National Field-Testing Facility (NFTF) at Ballina are analysed to predict the response of foundations under unconsolidated and undrained (UU) loading. Results of large-scale shallow foundation of UU tests are limited in the literature, and most of them were tested at UK's national soft soil test site in Bothkennar. To improve the accuracy of determining soil properties, a full-scale embankment, with both in situ and laboratory tests tools, was constructed and instrumented at Ballina in 2013. The instrumentations include measurement of horizontal and vertical loadings, deformations and pore pressure over time. Two rigid square foundations were loaded vertically to failure under UU condition. The foundation response is recorded and load- settlement graph indicates its bearing capacity behaviour.

It has been found that many bearing capacity theories are not rigorous and contain lots of uncertainties such as the boundaries between footings and excavation wall, slope height, or the soil properties. In recent twenty years, researchers explored professional software to solve complex geotechnical problems based on the development of the computer. The finite element analysis (FEA) is one of geotechnical modelling methods to investigate the specific issues. In this study, numerical analysis apply on Plaxis 2D is used to calculate the bearing capacity of footings. By using this software, a predicted load settlement response can be identified.

3.2 BACKGROUND OF THE SITE

The test site is located at Ballina in NSW, Australia as shown in the map in Figure 10. The site is founded to be 6.5 Ha in area and lies on the Richmond river. Through the observation of boreholes, the groundwater level is about 1.0 m depth (0.5m AHD). The site is comprised of 1.5 m of alluvial clayey sand, underlain by 11 m soft estuarine clay. Photo is shown in Figure 11. A comprehensive site investigation has been conducted by geotechnical engineers involving drilling 15 boreholes and collecting soil samples by test apparatus. A range of field tests have been conducted in the Figure 12, which include cone Penetration tests (CPT), triaxial

Compression (TC) & triaxial extension (TE) test, and self- boring Pressuremeter test (SBPMT). There are similarities existing between Bothkennar and Ballina site. For example, the site condition and foundation geometry are extremely similar for both sites. The Bothkennar site is comprised of 2 m of clay and silt, underlain by few meters marine clay. The observed foundations have similar dimensions and same testing procedures in order to compare the results of tests.

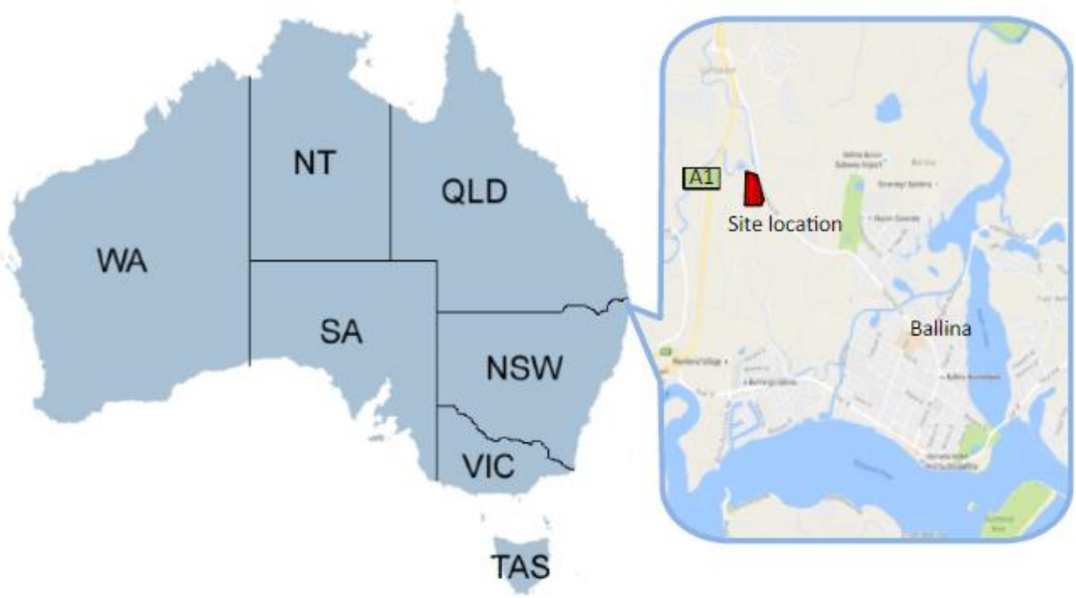

Figure 10. Site location (Science Direct, 2018)

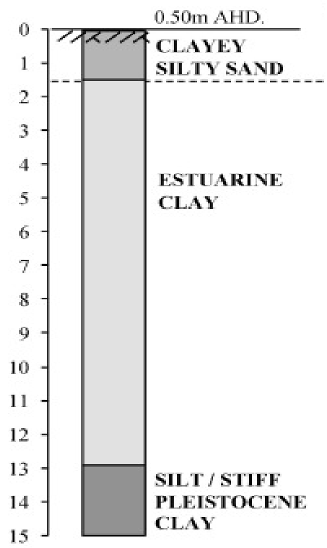

Figure 11. Foundation tests, Ballina region in NSW

Figure 12. Tests distribution (Ballina, 2013)

3.2.1 Foundation construction and loading blocks

The early stage of preparing testing apparatus include build and cast tested foundations and loading blocks. In this case, square foundations with 1.8 m length and 0.6 m thick were cast 1.5 m below ground level. The configuration and ground water level of footings is shown in Figure 13. The relevant excavating procedures include excavate a 2.4 × 1.5 m^2 construction space. After the excavation, the foundation was cast in concrete with 32 MPa and a surrounding timber formwork was built to against the concrete pressure. The loading blocks are made with same plan dimension of square foundations but 0.425 m height. Each reinforced concrete block has weight about 3.3 tonnes with average unit weigh of 24 KN/m^3, which indicates that each block led to an increasing of 10 KPa bearing pressure.

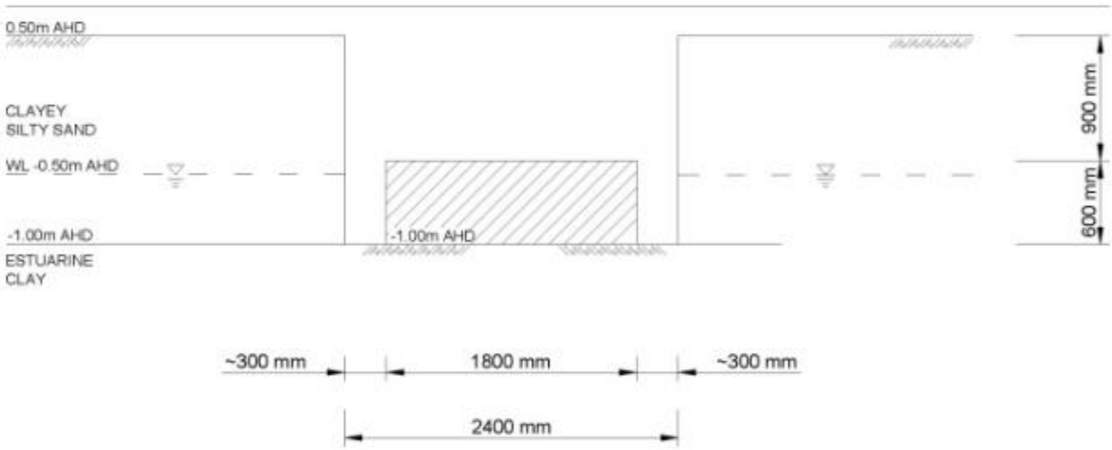

Figure 13. Square footing dimensions

3.3 UNDRAINED SHEAR STRENGTH RELATIONSHIP WITH ULTIMATE BEARING CAPACITY

Bearing capacity is defined as the capacity of the soil to support the foundation. To calculate the ultimate bearing capacity, it is important to find the soil properties through in situ tests and laboratory tests. The soil parameters such as strength, stiffness and permeability can be determined through these tests. In this case, a modified Terzaghi's bearing capacity equation is used to represent the undrained shear strength and its relationship to bearing capacity.

$$Q_u = \text{A}\,(N_c S_u + qN_q) \quad (25)$$

Where A = Area of the foundation, N_c, N_q = bearing factor, q= surcharge adjacent to the foundation

The Terzaghi's bearing capacity factor is related to the internal friction angle. In undrained condition, the increase in pore pressure occurs at the same rate as the application of stress. Therefore, the internal friction angle ($\emptyset$) is equal to zero, which leads to N_c = 6 and N_q = 0 from chart. A straight relationship between ultimate bearing capacity and undrained shear strength can be obtained for this case.

$$Q_u = 19.44 S_u \quad (26)$$

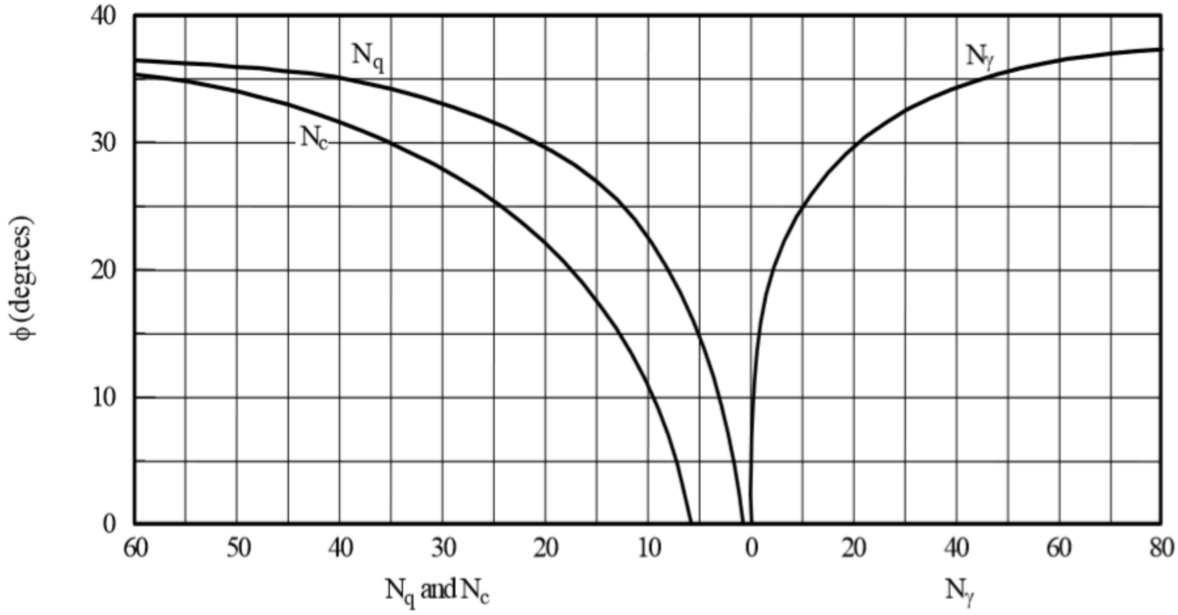

Figure 14. Bearing capacity factor (Terzaghi and Peck, 1948)

Undrained shear strength can be estimated through a range of in situ and laboratory tests, which include CPT, SBPM, TXC and TXE tests.

3.3.1 Undrained shear strength for Cone penetration tests

Geotechnical parameters can be estimated in cone penetration tests depending on soil types. These parameters include total cone resistance, penetration pore pressure, empirical cone factor. The total cone resistance is shown in the following equation,

$$q_t = q_c + (1\text{-a})\, u_2 \tag{27}$$

Where, q_t = total cone resistance, q_c = Cone resistance, u_2 = penetration pore pressure

The undrained shear strength can be calculated in terms of the cone resistance and empirical cone factor.

$$S_u = (\, q_t - u_2 \,) \,/\, N_k \tag{28}$$

Where, S_u = undrained shear strength, N_k = empirical cone factor

3.3.2 Undrained shear strength for self-boring pressuremeter test

Various methods have been used for calculating undrained shear strength for pressurementer tests. Most common method is to use Gibson & Anderson (1961) approach for interpreting a Menard pressuremeter test (Gaone, 2016). Undrained shear strength can be simplified as a gradient of cavity pressure against logarithm of the cavity strain.

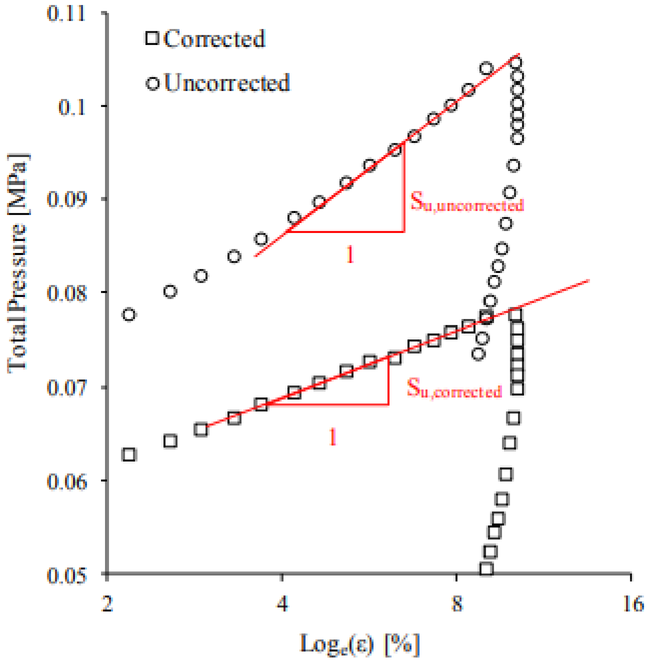

Figure 15. Example of undrained shear strength for SBPM

3.4 SOIL STIFFNESS AND ITS RELATIONSHIP TO SETTLEMENTS

In this section, shear modulus can be determined through Triaxial compression tests and self-boring pressuremeter tests. Shear modulus is determined as the rate of shear stress to the shear strain. It is an important factor to observe the deformation of foundations. By selecting three significant points on deviatoric stress (q) versus axial strain ($\mathcal{E}_a$) graph- $G_{10}, G_{50}, G_{MCCtx}$, best fit linear shear modulus versus depth graph can be obtained. Each point represents 10%, 50% and optimized of the total change in deviatoric stress. Figure 16 shows one example of triaxial compression test data at 4.75 m depth. Three points for stress-strain rate with varies depth are applied to generate the shear modulus versus depth graphs.

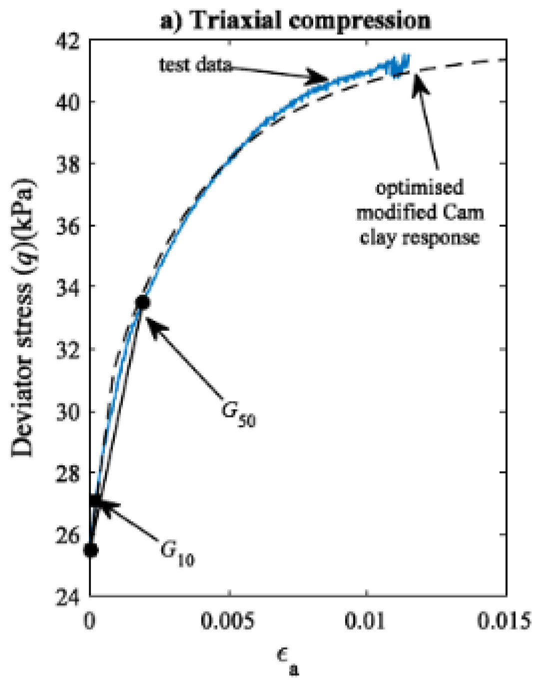

Figure 16. Deviatoric stress-strain graph for TC (Doherty, 2018)

Since the foundation is embedded below 1.5 m of ground surface, a transfer equation created by Doherty and Deeks for shallow foundation were used to calculate the shear modulus at 1.5 m.

$$G(z) = G_R \left(\frac{Z}{R}\right)^{\alpha} \quad (29)$$

Where, G_R is shear modulus at depth equal to the radius of foundation, α is the non-homogeneity parameter

Doherty and Deeks (2003) also developed a graph to estimate stiffness coefficients such as non- homogeneity parameter and vertical stiffness coefficients. To predict the relevant data, Poisson’s ratio should be determined first using site investigation techniques. In this case, Poisson’s ratio = 0.5 and ratio of depth to radius = 1.5. Figure 17 shows the estimation results for soil stiffness data.

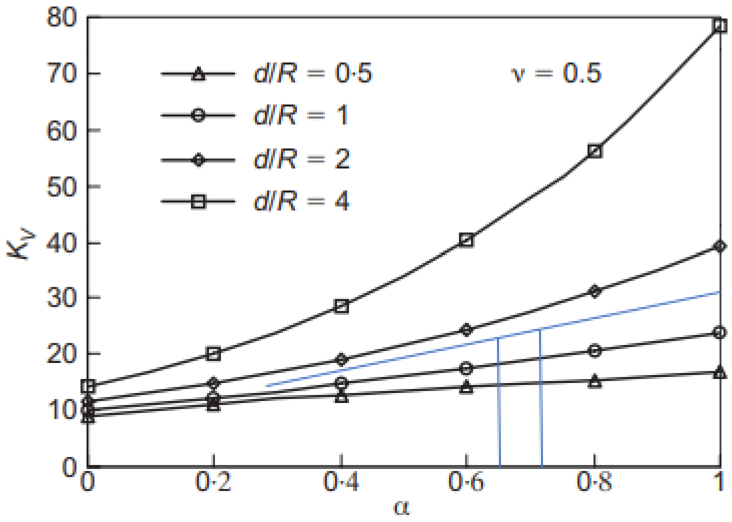

Figure 17. Soil stiffness graph for Poisson's ratio at 0.5 (Doherty and Deeks, 2003)

3.4.1 Vertical settlement

In this section, total settlement can be estimated once the above parameters are obtained.

$$U = \frac{Q}{G_R \mathrm{R} K_v} \tag{30}$$

Where, U = Total vertical settlement, Q= ultimate bearing capacity, R = radius of foundation, K_v = vertical stiffness coefficients

Once the settlement is calculated, it is supposed to find efficient settlements under working loads. The total vertical settlement is significantly affected by inefficient loading after failure. To investigate the reasonable load-settlement response, settlements of 25%, 50% of ultimate failure load (u_{25}, u_{50}) are estimated.

3.5 FINITE ELEMENT ANALYSIS (FEA)

A suitable foundation design requires reasonable estimation in terms of soil properties, ultimate bearing capacity, and interaction between footing geometry and soil parameters. Therefore, it is essential to identify numerical analysis inputs efficiency to avoid unexpected results. In this case, Plaxis 2D is used to simulate the square footing behaviour in unconsolidated undrained condition. An axisymmetric model using 15-noded elements was created. The two different layers of soil with 1.5 m clayey sand and 8.5 m estuarine clay was modelled to represent the crust and underlaying soils. The excavation and foundation geometry are shown in Figure 18.

The axisymmetric model simulates the foundation and excavation pit as circle, which means the boundaries of both pits can be calculated as radius. The foundation and excavation have radius of 1.013 m and 1.35m, which has a gap about 0.34m.

3.5.1 Material input

Material input includes determination of material model, soil unit weight, Young’s modulus, undrained shear strength. The crust layer was selected as a Mohr- Coulomb model, which is also called linear elastic perfectly model. Mohr-Coulomb model is based on Hook’s law of isotropic elasticity, which relate the stress rate to the elastic strain rates. This is shown in Figure 18. The strain rates can be either elastic or plastic. The Young’s modulus 3MPa and undrained shear strength 24 kPa are obtained through CPT. The average unit weight of sand is 17 KN/m^2, Poisson’ ratio is determined as 0.495 (0.5) for undrained material due to the strain is small enough. Similar as crust layer, the soft clay was modelled as a Tresca elastic plastic model with 8.5 m thickness. The unit weight is 14 KN/m^2, and 11.2 kPa as undrained shear strength.

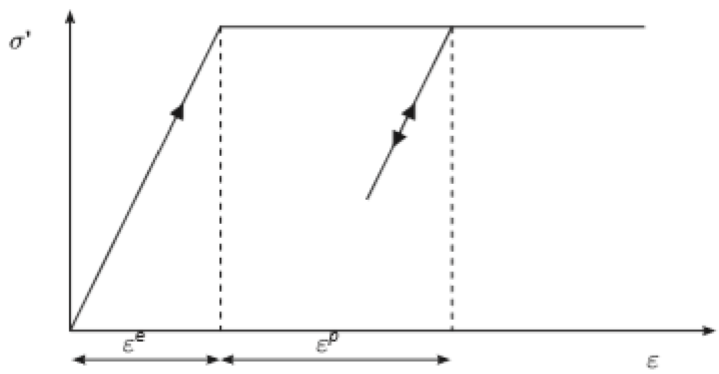

Figure 18. Elastic perfectly model (Plaxis 2D, 2018)

3.6 PROJECT TIMELINE MANAGEMENT

In this section, a detailed timeline for the project is discussed to conduct the project in a realistic and feasible way. Since the project consists of few activities, such as topic selection, proposal presentation, literature review, supervisor meeting, Expo poster etc, it is important to report each period progress to make sure the whole project can be accomplished on time. The project starts from March of 2018 and finishes at 15th of October. It includes Project proposal presentation, literature investigation, Project results presentation, Expo poster, and final thesis. However, the project takes almost nine months to complete. During this period, the time management is necessary for student to update realistic course performance.

In semester 1, the task was focused on the selection of project topic and feasibility studies. After selecting the project topic and identifying the reliability of the references, a proposal presentation on mid break of semester one. This presentation contains a feasibility study of current state of knowledge and make students understand the project plan of task in next semester. Student is supposed to finish their literature review by the end of semester one.

In semester two, the study focuses on experimental results such as empirical hand calculation results and numerical analysis results. It is supposed to meet with supervisor once a week to solve questions. Since this project has no experimental tasks, the major work focuses on theoretical performance, which include investigate geotechnical issues relevant to given in situ and laboratory data and Plaxis 2D (numerical analysis). A project results presentation is planned to be presented in week 7 to evaluate the understanding of the topic. In the presentation, students are supposed to display their investigation results to audience and prove why it is worth to do this topic. An Expo Poster is necessary to be finished in week 11. Meanwhile, the edition of the final report is supposed to be done.

Table 2.

Project timeline

Tasks Name	Duration (days)	Start	Finish
Project selection	12	26/02/18	10/03/18
Proposal presentation	30	10/03/18	10/04/18
Literature review	18	10/04/18	21/07/18
Case study investigation	70	21/07/18	14/09/18
Results seminar	2	17/09/18	18/09/18

Optimization results data	10	18/09/18	28/09/18
Expo Poster	2	16/10/18	17/10/18
Final thesis submission	61	15/08/15	15/10/15

4 BALLINA CASE RESULTS

In this part, details of the case study results are shown both hand calculation and numerical results. The first part of results includes Terzaghi's bearing capacity calculation in terms of foundation settlement. The second part of results indicate numerical model of load- settlement response by finite element analysis. Meanwhile, both empirical results and numerical results would compare with the measured foundation performance values (UU data).

4.1 RESULTS OF UNDRAINED SHEAR STRENGTH

Undrained shear strength can be obtained from a couple of in situ tests and laboratory tests. These tests include triaxial compression test (TC), triaxial extension test (TE), cone penetration test (CPT) and self- boring pressuremeter test (SBPM).

4.1.1 Undrained shear strength for CPT

Table 3 shows the results of undrained shear strength with varies depth in cone penetration test. Undrained shear strength is calculated by using rate of effective cone resistance and given empirical cone factor. Figure 19 shows the undrained shear strength versus depth graph for CPT. The linear line is plotted to represent the trend of graph and also helpful to find the undrained shear strength at foundation level (1.5 m below the ground surface). For the CPT profile, the empirical cone factor is given as 12.2 from in situ test data (Kell, 2014).

$$S_u = (q_t - u_2) / N_{kt} \qquad (31)$$

Where S_u = Undrained shear strength, $(q_t - u_2)$ = Effective cone resistance,
N_k = Empirical cone factor

The depth of soil depends on the thickness of layers. In this case, the first layer is clayey silty sand with 1.5 m thickness and second layer is estuarine clay about 12 m. Based on the excavating level at 1.5 m below the ground, the total 10 meters depth is enough for site investigation.

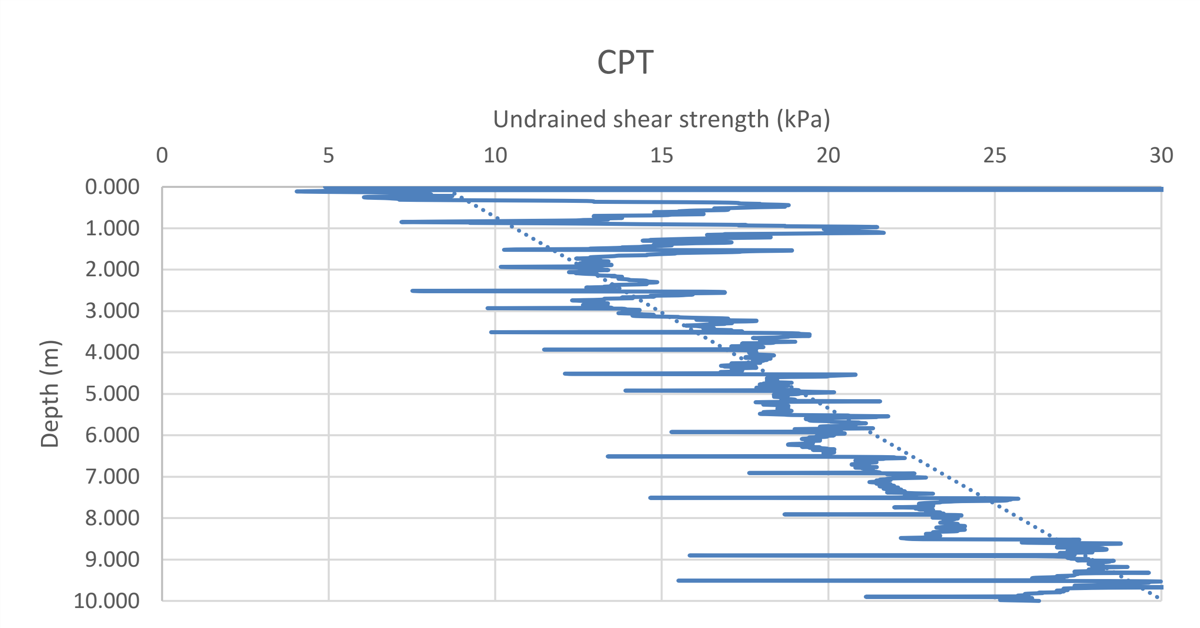

Figure 19. Undrained shear strength profile for CPT

4.1.2 Undrained shear strength from TC and TE

The triaxial compression and triaxial extension tests data are given below. In an unconsolidated undrained condition, the friction angle is zero due to the effective stress will always be the same. The best linear line graph related to undrained shear strength with depth are shown in Fig 20 and Fig 21.

Table 3.

Undrained shear strength data for TC

Depth (m)	Unconfined compressive strength (KPa)	Undrained shear strength (KPa)
D	q_u	$S_u = q_u / 2$
1.76	14.6	7.3
1.96	18.5	9.25
2.37	27.24	13.62
3.05	23.44	11.72

4.76	22.78	11.39
4.96	28.46	14.23
5.4	26.22	13.11
5.58	29.12	14.56
6.53	30.06	15.03
7.38	8.72	17.44
7.88	34.3	17.15
10.34	33.6	16.8

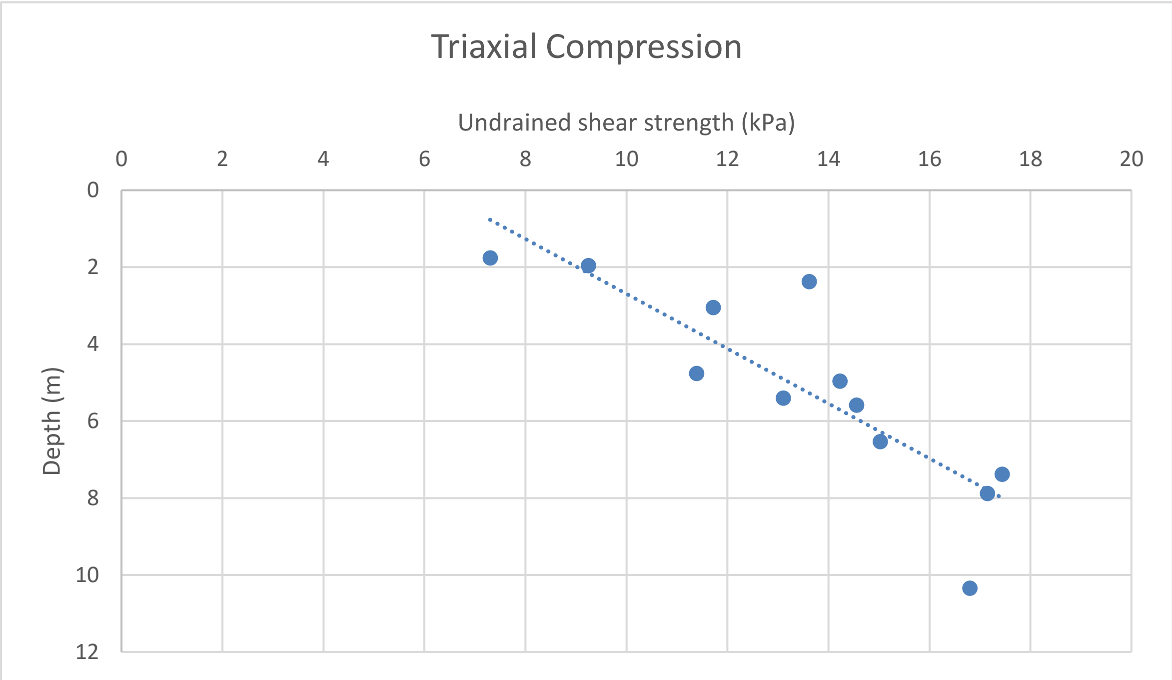

Figure 20. Undrained shear strength profile for TC

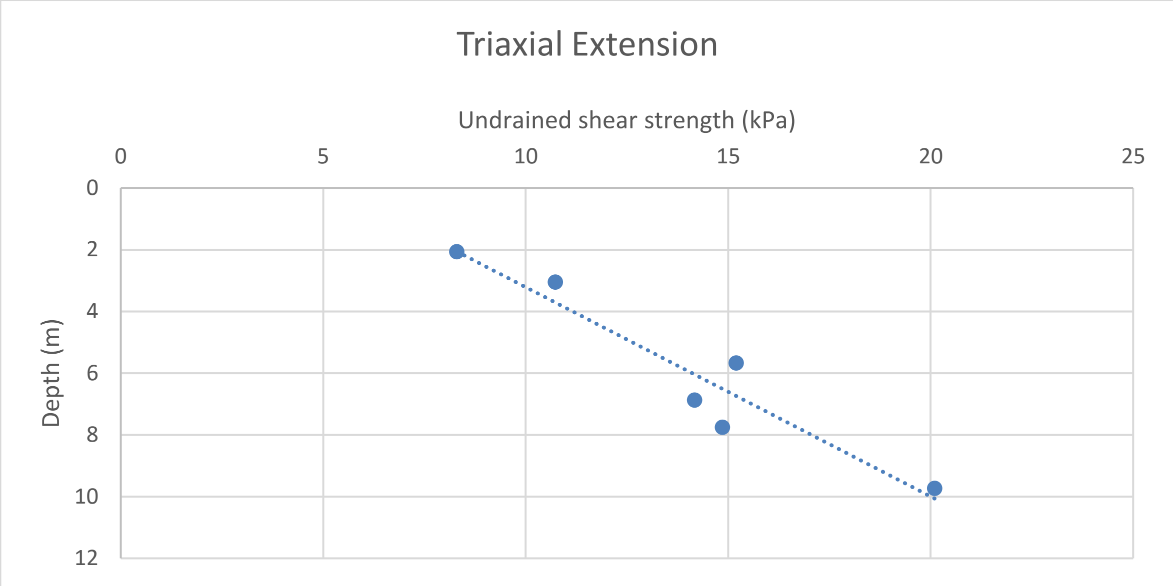

Figure 21. Undrained shear strength profile for TX

4.1.3 Undrained shear strength for pressuremeter test

The undrained shear strength for SBPM can be determined in elastic plastic model following by Gibson & Anderson (1961) approach. Undrained shear strength is the gradient of cavity pressure to logarithm cavity strain. The following graph shows the undrained shear strength profile at depth 2.15 m below ground surface. Figure 22 represents the shear strength versus depth graph, which S_u at foundation level is estimated as 10 KPa.

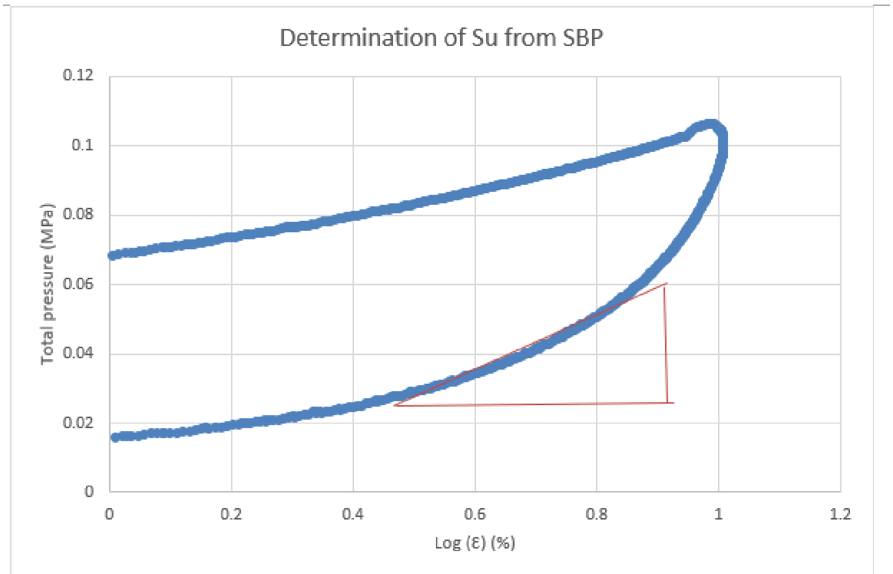

Figure 22. Undrained shear strength profile for SBPM at 2.15m

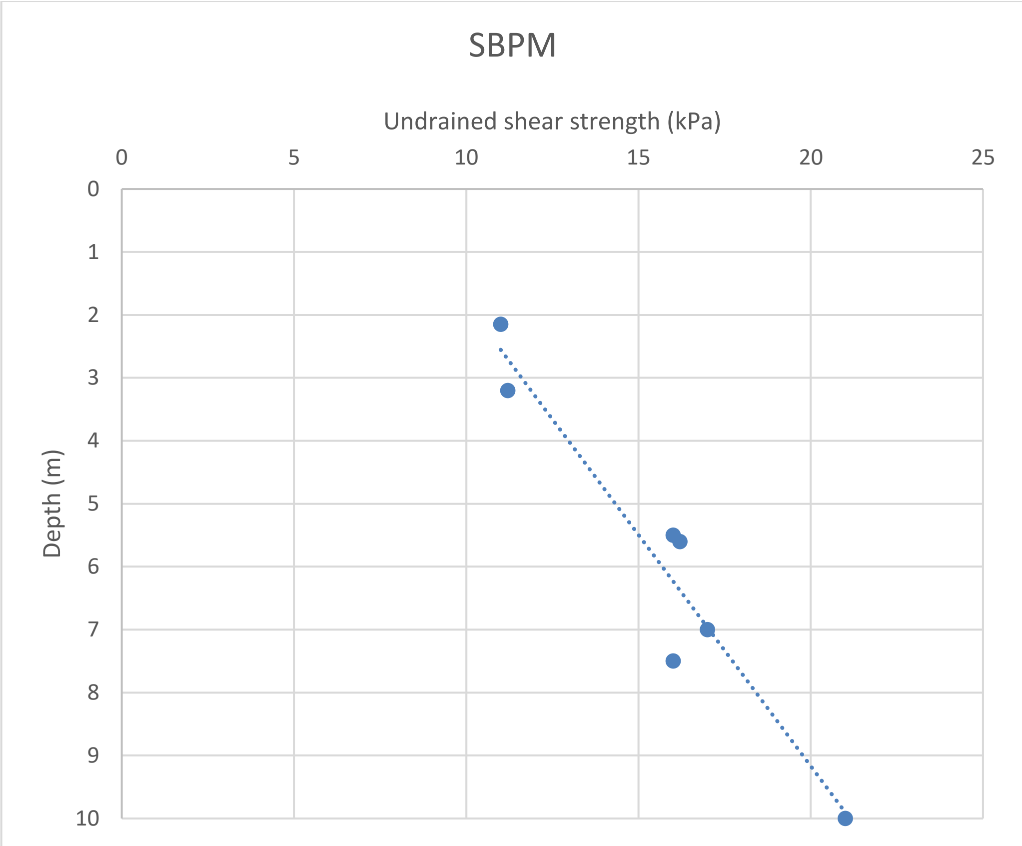

Figure 23. Undrained shear strength versus depth for SBPM test

4.1.4 Ultimate bearing capacity for each type of test

From section 3.3, the ultimate bearing capacity has a proportional relationship Q_u = $19.44S_u$. Table 4 shows the ultimate bearing capacity for each type of tests

Table 4.

Ultimate bearing capacity for each type of test

	TC	TE	SBP	CPT
S_u (kPa) at 1.5 m	8.5	8	10	11
Q_u (KN) at 1.5 m	165	156	194	214

4.2 RESULTS OF SHEAR MODULUS AND SETTLEMENT

This section covers the shear modulus and foundation settlement results for Ballina case. The shear modulus can be estimated from TX and SBPM with multiply methods. The foundation settlement found following a relationship with shear modulus, ultimate bearing capacity and stiffness coefficients.

4.2.1 Shear modulus results for triaxial test

The interpretation of soil stiffness has shown in section 3.4. Three significant points G_{10}, G_{50}, G_{MCCtx} represents the percentage of the total change in deviatoric stress. Figure 24 shows the elastic shear modulus from stress- strain graph at depth 4.75 m. By using the stress- strain theory, three stiffness values for varies depth are plotted. Following the same procedures, shear modulus at varies depth can be calculated in Table 4. Figure 25, Figure 26 and Figure 27 represents the linear line trend of shear modulus at each point. After that, soil stiffness at foundation level 1.5 m can be estimated.

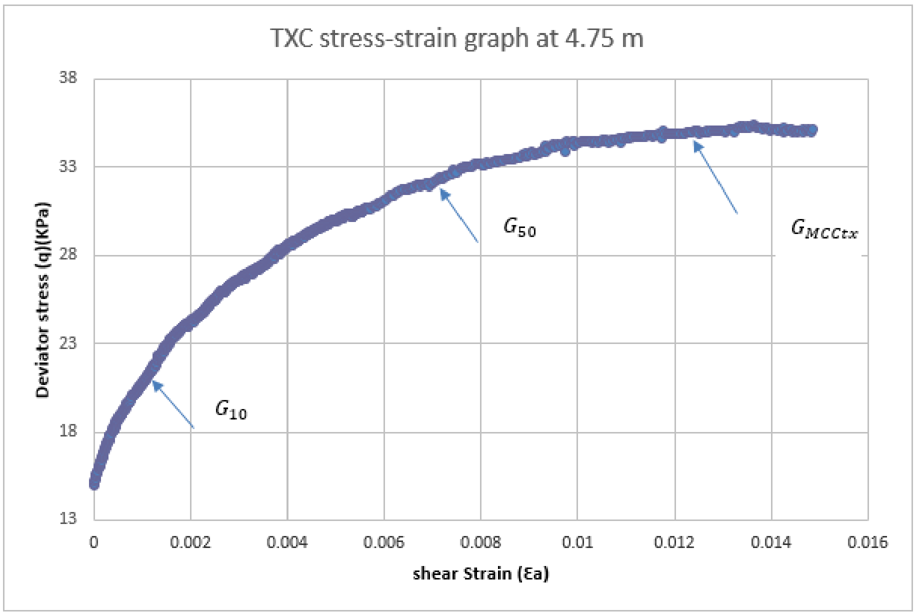

Figure 24. Shear modulus profile for TX at depth 4.75m

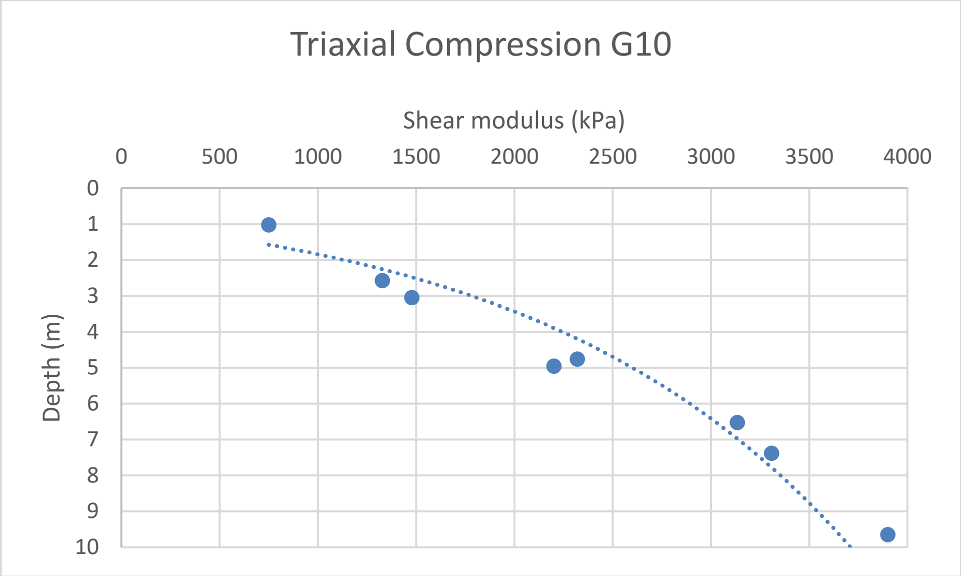

Figure 25. Shear modulus G_{10} profile

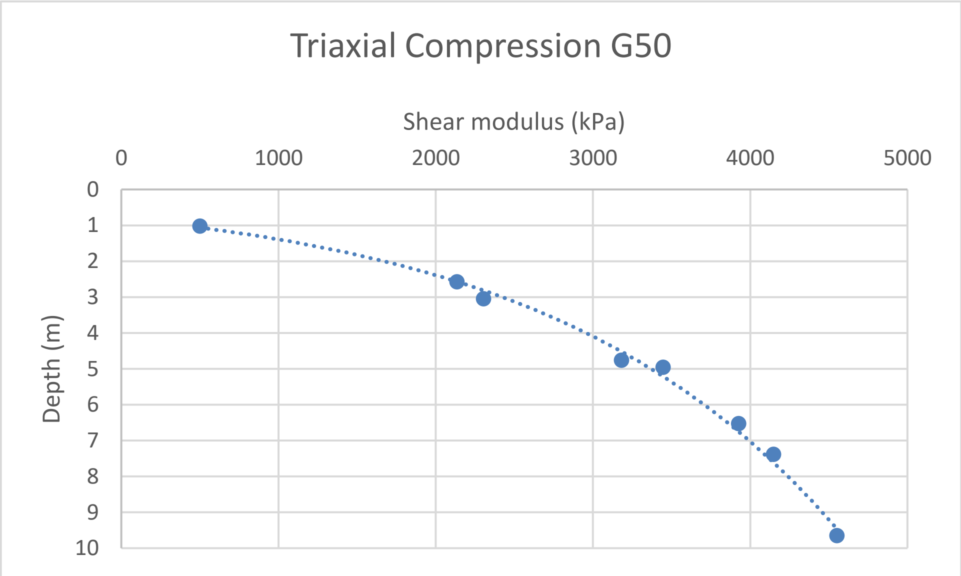

Figure 26. Shear modulus G_{50} profile

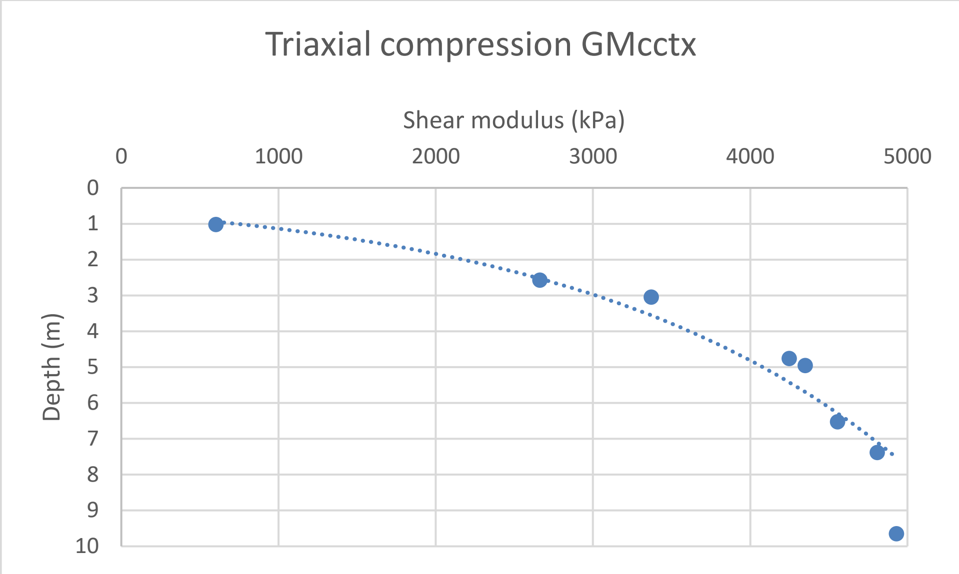

Figure 27. Shear modulus G_{Mcctx} profile

Table 5.

Soil stiffness profile

Depth (m)	G10 (kPa)	G50 (KPa)	G_{MCCtx} (KPa)
1.76	570	1370	1814
2.57	1327	2133	2662
3.05	1477	2302	3370
4.76	2320	3180	4248
4.96	2200	3445	4350
6.53	3134	3926	4555
7.38	3309	4147	4808
9.65	3900	4550	4930

4.2.2 Shear modulus results for SBPM

The shear modulus for SBPM can be determined from the stress-strain curve. Figure 28 represents the cavity pressure versus strain at depth 2.15m, 3.2m and 5.5m. Shear modulus can be determined by an unload- reload loop carried out at a nominated cavity strain.

$$G = \frac{1}{2}\frac{dp}{d\varepsilon} \tag{32}$$

Where, G = shear modulus, $\frac{dp}{d\varepsilon}$ = the gradient of total pressure to cavity strain

Shear modulus at three depth are 1020 kPa, 1240 kPa, 1480 kPa. A linear trend line can be created to estimate the shear modulus at foundation level 1.5 m. This is shown in Figure 29.

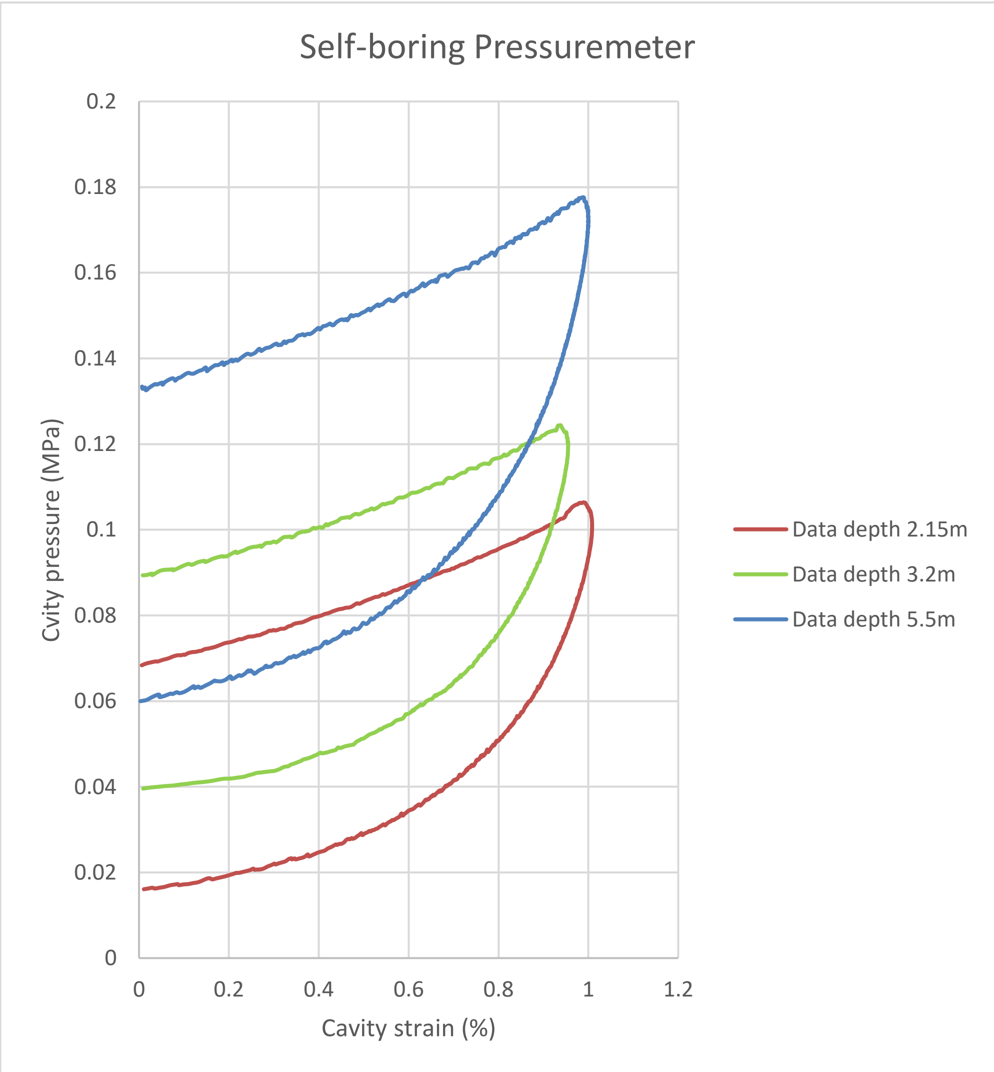

Figure 28. Pressuremeter data at varies depth

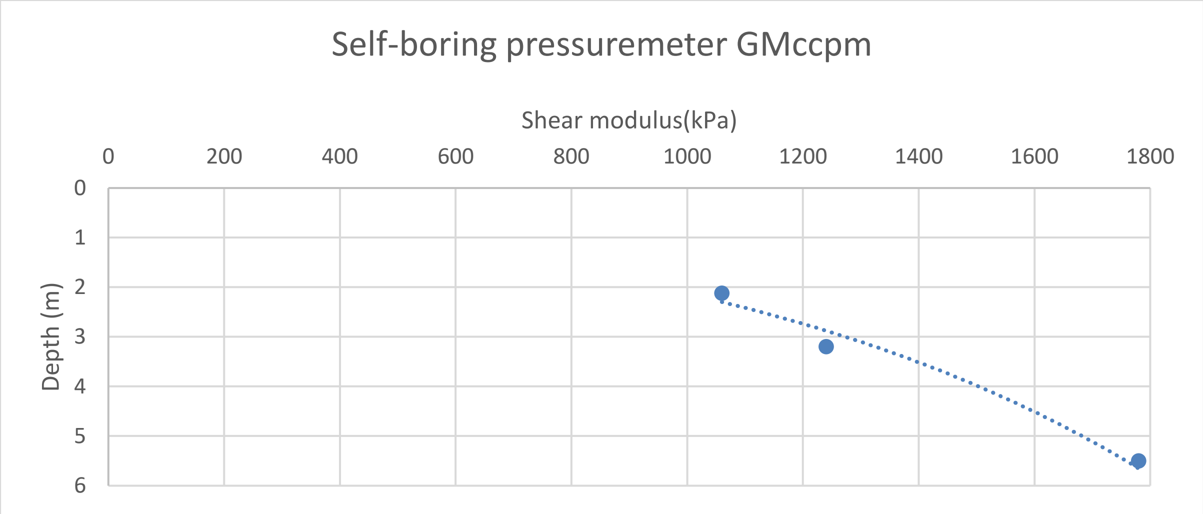

Figure 29. Shear modulus for SBPM

4.2.3 Results of elastic shear modulus

Since the soil stiffness for each type of test is calculated, Eq. (29) from Doherty and Deeks (2003) is used to solve elastic shear modulus problems. Doherty and Deeks investigated the shallow foundation of circular and transferred soil stiffness to foundation shear modulus. Table 6 shows the shear modulus at foundation level. TX has shear modulus of 1100 kPa, 1200 kPa and 1600 kPa at percentage of total deviatoric stress- strain rate respectively. Shear modulus of SBPM has 1000 kPa at foundation level.

Table 6.

Shear modulus for each type of test

	G_{10}	G_{50}	G_{MCCtx}	G_{MCCpm}
$G_{1.015}$ (kPa)	750	500	600	700
$G_{1.5}$ (kPa)	1100	1200	1600	1000
α	0.7	0.65	0.7	0.7
K_v	22.1	20.9	22.1	22.1

4.2.4 Results of foundation settlement

As discussed in section 3.4.1, the efficiency settlements under working loads are estimated to investigate load- settlement response. For serviceability design, settlements at 25%, 50% of ultimate failure load (u_{25}, u_{50}) are investigated.

Table 7.

Foundation settlements for TX and SBPM

	G_{10}	G_{50}	G_{MCCtx}	G_{MCCpm}
$G_{1.015}$ (kPa)	750	500	600	700
u_{25} (mm)	3.04	4.8	3.8	3.3
u_{50} (mm)	6.1	9.7	7.6	6.5
u_{100} (mm)	12.2	19.3	15.3	13.1

The load-settlement graphs for each soil stiffness are shown in Figure 30. The blue curve represents the measured foundation performance for unconsolidated undrained test (UU). The measured UU test has settlement and ultimate failure load in Table 8. The settlement at 25%, 50% and 100% of failure load is 3mm, 6mm and 22 mm respectively. In Figure 30, it can be found that the G_{10} and G_{MCCpm} has a remarkable prediction for u_{25} and u_{50} compare with UU tests. The soil stiffness for TX- G_{MCCtx} also has a good estimation for u_{25} and u_{50}. While most of types have different values for ultimate settlement.

Table 8.

Foundation performance for UU test

	Measured Values
Failure Load Q (KN)	205
u_{25} (mm)	3
u_{50}(mm)	6

u_{100}(mm)	22

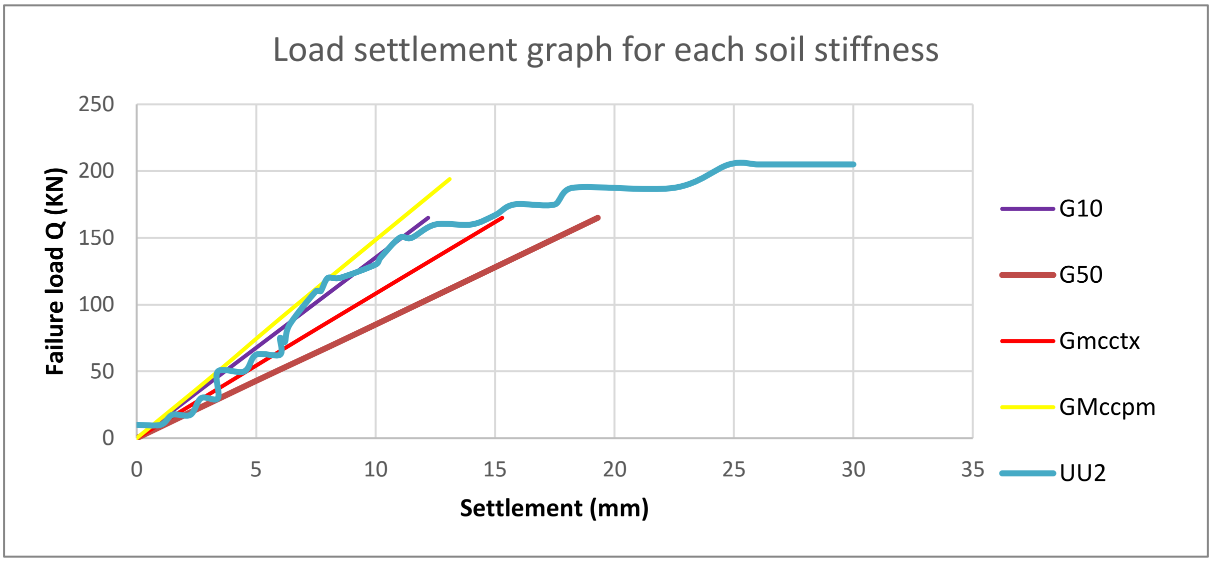

Figure 30. Load settlement for each soil stiffness

4.2.5 Results of FEA

In this section a Tresca soil model was simulated by geotechnical software- Plaxis 2D to analyse the soil behaviour of foundation in Ballina. The material input data has been discussed in section 4.5. The crust layer is clayey silty sand with 1.5 m thickness, underlay by 8.5 m thickness of estuarine clay. The GW is 1 m below the ground surface. This is shown in Figure 31. To consider the horizontal deformation of crust, the axis boundary should be long enough to avoid unexpected soil collapse. Therefore, 30 m is used for soil layer length.

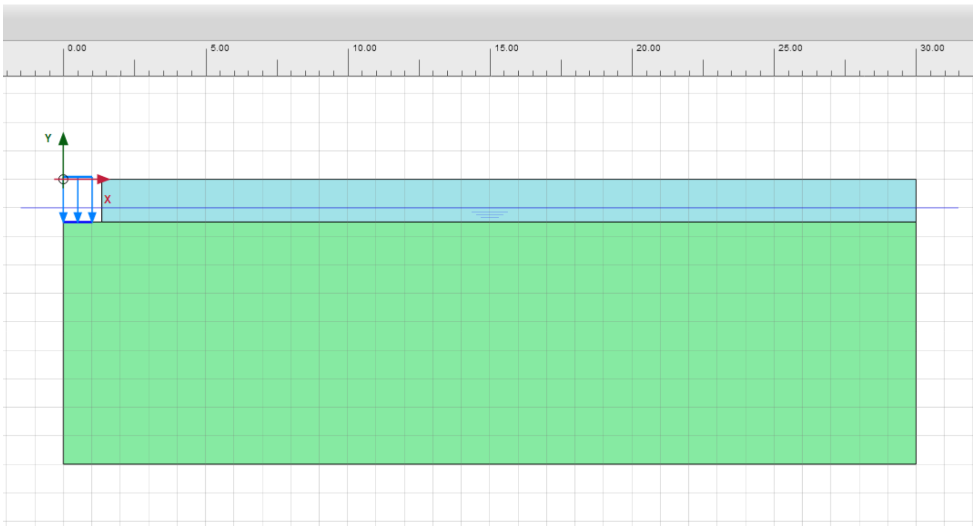

Figure 31. Plan view of FEA model

The model set the dimensions of square foundation and excavation pit as circle. Therefore, the foundation and excavation pit have radius of 1.013 m and 1.315 m. The simulation stage consists of two steps, which include excavates a 1.315m width and 1.5 m depth pit, creates a in situ footing with cumulative load until failure. In reality, each concrete block has a weight about 3.3 tonnes with a unit weight of 24 KN/m^2, which represents that each block increases the pressure about 10 kPa. Figure 34 shows the finite element mesh once the geometry setting is completed. Figure 33 shows the failure mechanism of FEA. It can be found that the failure happened surrounding by footings and the horizontal deformation can be neglected. The failure mechanism indicates that the clayey silty sand forced the deformation happened in the gap between footing and excavation wall. The crust is strong enough to make this phenomenon occur.

Figure 34 shows the load settlement response of model compare with the UU test. It can be found that FEA model provides a reasonable fit to the measured values performance. The settlement values of u_{25} and u_{50} are close for both curves.

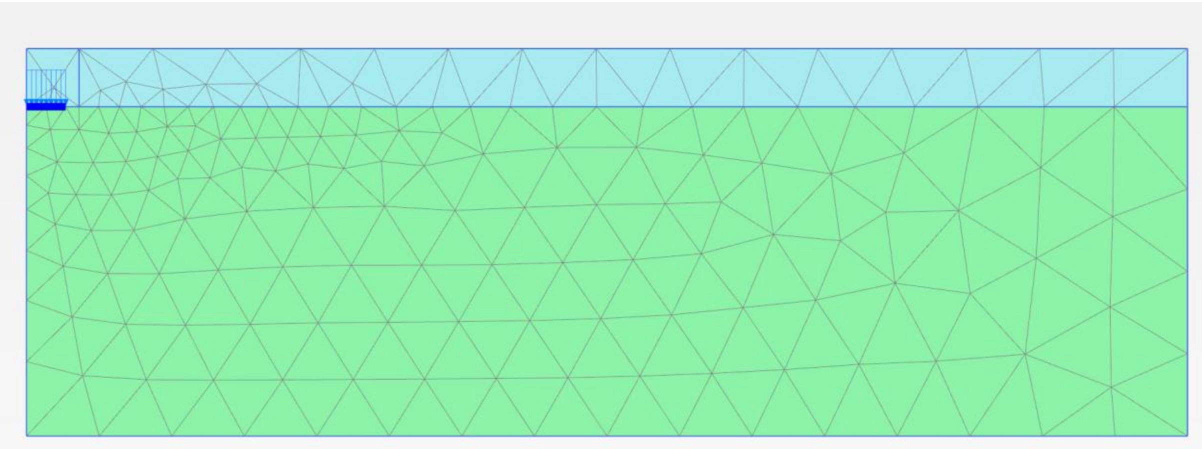

Figure 32. Mesh generating for FEA model

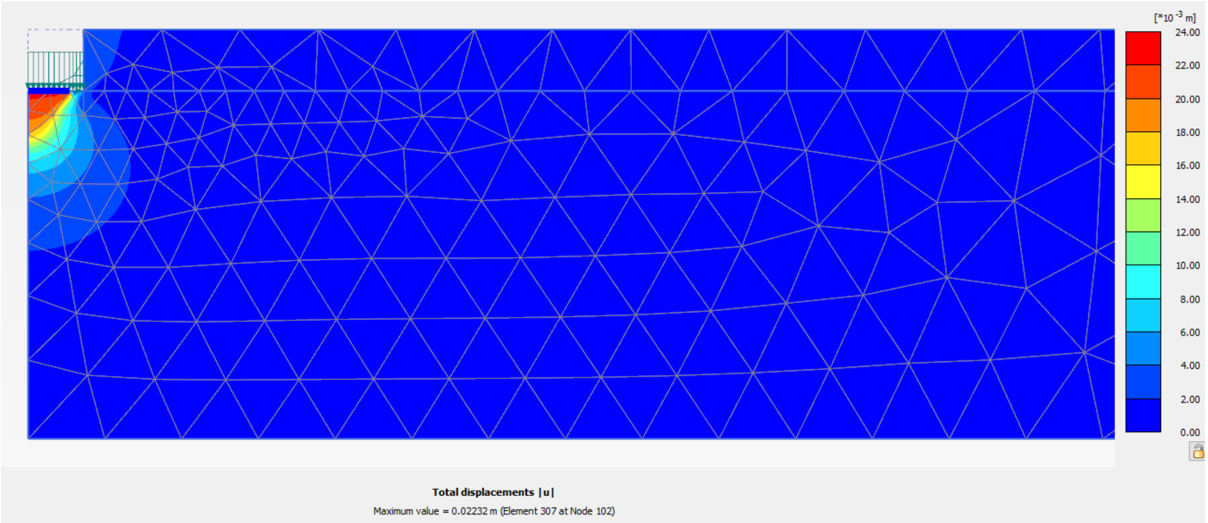

Figure 33. Total deformation of foundation

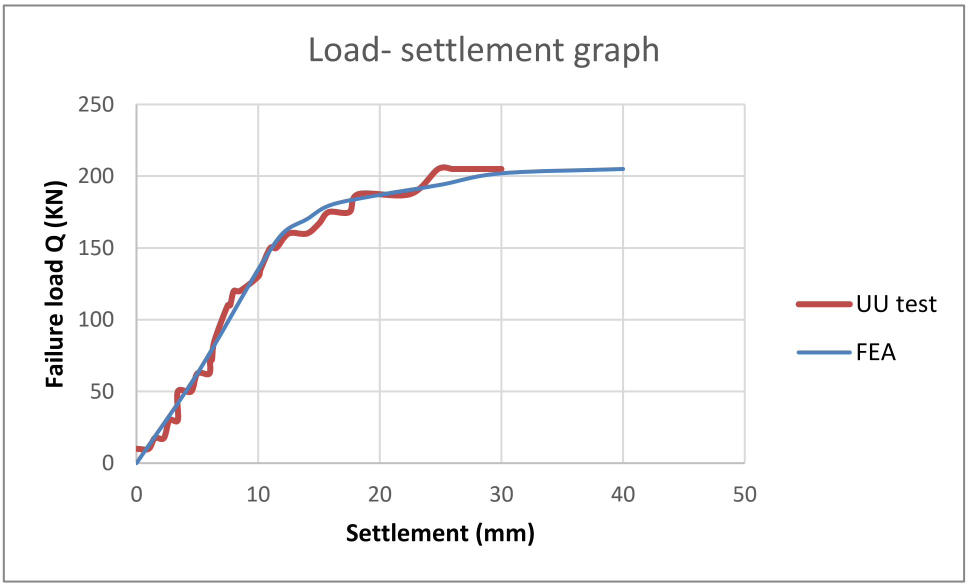

Figure 34. FEA load-settlement graph

5 ANALYSIS AND DISCUSSION

5.1 UNDRAINED SHEAR STRENGTH AND SETTLEMENT

The computed undrained shear strength and ultimate bearing capacity are given in Table 9. The measured values of foundation performance present in Table 9 to compare with each type of test. It has been observed that the undrained shear strength error ranges from 0- 20%, the bearing capacity error range from -24% to 4.3%. SBPM is a powerful apparatus to predict the undrained shear strength and ultimate bearing capacity within 5% error range. The CPT has a reasonable estimation for bearing capacity within an error range of 4.3%. It has also been observed that triaxial extension test always under estimate the shear strength and bearing capacity and triaxial compression test over-estimate the undrained shear strength.

Table 9.

Comparison of undrained shear strength and bearing capacity a foundation level

	TC	TE	SBP	CPT
S_u (kPa) at 1.5 m	10.5	8	10	11
% error Compare with 10 KPa	5	20	0	10
Q_u (KN) at 1.5 m	165	156	194	214
% error Compare with 205 KN	-19.5	-23.9	-5.3	+4.3

The computed settlement for each stiffness profile is shown in table below. It can be seen that G_{10} and G_{MCCpm} can reasonable estimate the foundation settlement at 25% and 50% of ultimate bearing capacity. G_{MCCtx} also provides a good estimation at same range. It can be summarised that undrained triaxial compression test is a good method to predict the elastic settlement subject to typical working loads.

Table 10.

Settlement for secant shear modulus

	G_{10}	G_{50}	G_{MCCtx}	G_{MCCpm}	UU test
u_{25} mm	3.04	4.83	3.81	3.26	3
u_{50} mm	6.1	9.7	7.6	6.5	6
u_{100} mm	12.2	19.3	15.3	13.1	22

5.1.1 Load settlement response for empirical and numerical methods

The load- settlement response for triaxial compression and self- boring pressuremeter test is shown in Figure 35 and compared with measured foundation performance and finite element model. It was demonstrated that the non-linear finite element model can match the measured foundation response. Both reasonable bearing capacity and settlement can be achieved using a perfectly linear elastic soil model. It is important to determine the input data for numerical model to achieve the correct response. In numerical analysis, the undrained shear strength for Triaxial compression test and secant shear modulus (G_{10}) are used to simulate the model.

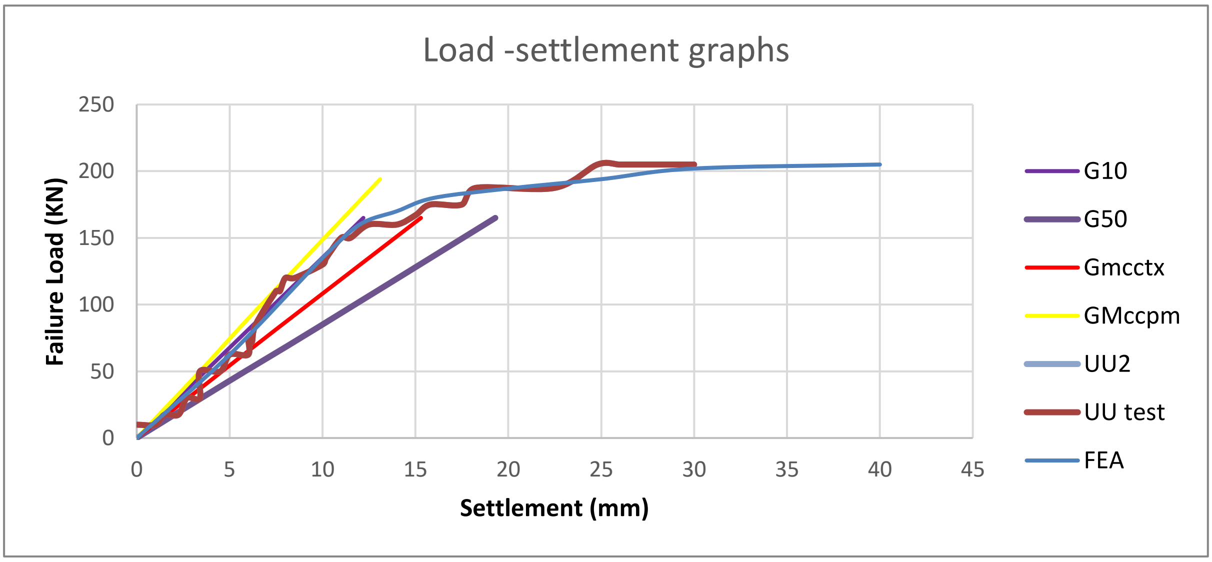

Figure 35. Load- settlement graph for hand calculation and numerical analysis

5.2 BOUNDARIES IMPACT FOR NUMERICAL ANALYSIS

In this section, the effect of gap between foundation and excavation wall will be investigated. In Fig 36, the failure condition occurred around footings, extending only to the edge of excavation wall. The gap between footings and excavation wall can significantly impact the load settlement response for FEA analysis. Fig 37 shows the foundation embedded with no gap. It was found that the impact of deformation extends to the edge and part of stress loads on the excavation wall. The total settlement reduces from 22 mm to 12 mm and ultimate failure load increase up to 50% compared with original model. A non-linear graph in Fig 38 shows the impact of the gap between footing and stand wall. The Y-axis represents the rate of ultimate failure load. It was found that the increase of gap would over-predict foundation's ultimate bearing capacity.

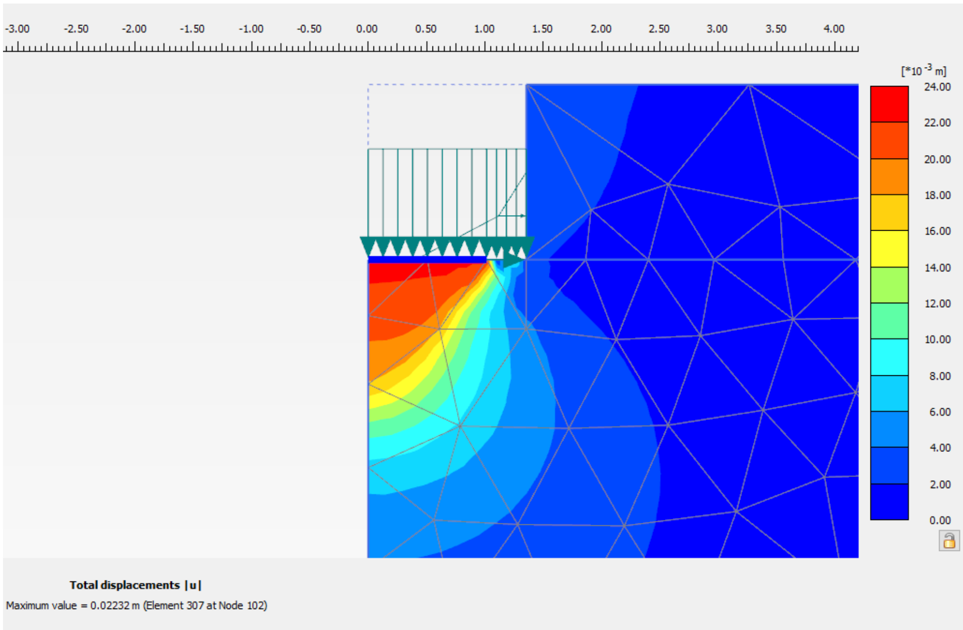

Figure 36. Failure mechanism for g=0.34 m

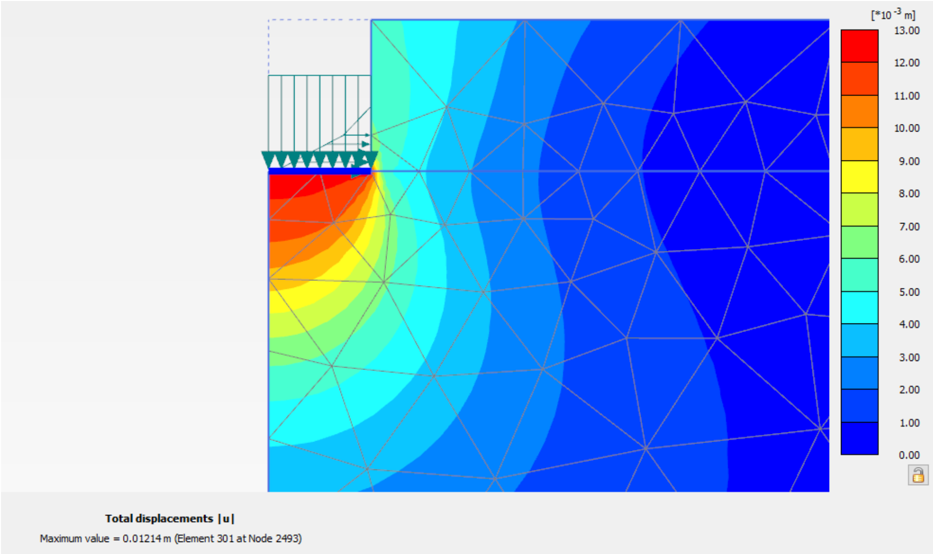

Figure 37. Failure mechanism for g=0 m

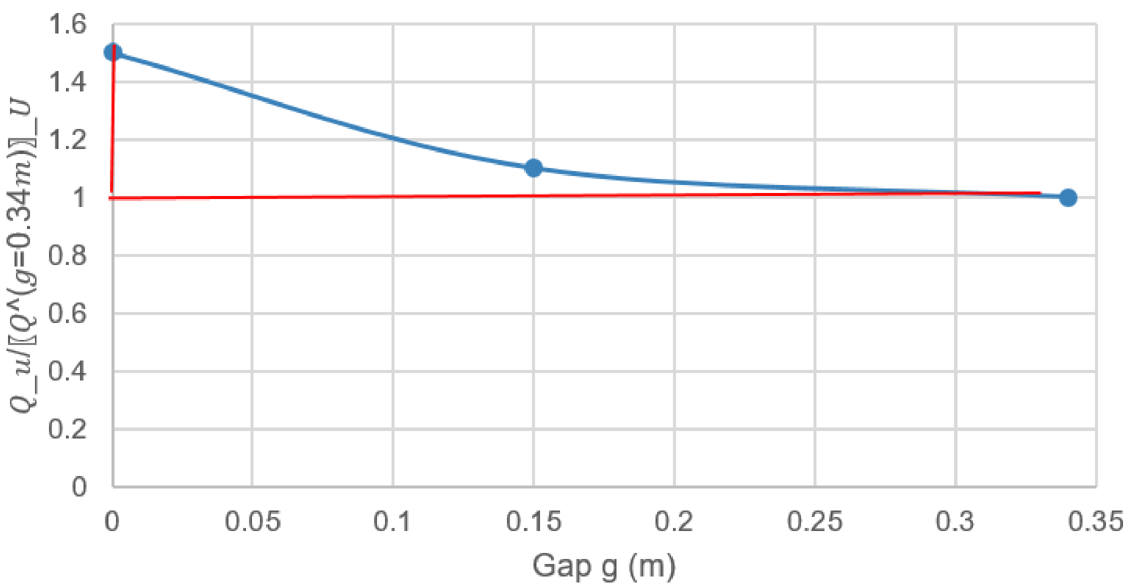

Figure 38. Impact of the gap to calculate bearing capacity

5.3 BEARING CAPACITY EQUATIONS FOR UNDRAINED CLAY

In this section a variety of bearing capacity equations for undrained clay are discussed to find the factors that impact ultimate bearing capacity. The oldest and simplest method for estimating bearing capacity for undrained clay is limit equilibrium back to the time of beginning of 20th. This approach prsumes a failure mechanism and assumes stress on the failure planes are limited by undrained shear strength (C_u) and internal friction angle (θ). This theorem combines both lower and upper bound analysis for bearing capacity estimation. In this case, the exact solution for limit equilibrium is derived from $4C_u \leq$ q $\leq 5.52C_u$ and is given by Prandtl (1921) as q = (2+π) C_u = $5.14C_u$

Table 11.

Prandtl's equation data

Prandtl's estimation of bearing capacity Q= $5.14C_u$	Undrained shear strength c_u (KPa)	Ultimate bearing capacity (KPa)	Failure Load (KN)
	10	51.4	166

The measured failure load is 166 kN, which is 19% less than the expect failure load 205 kN. This method has disadvantage of considering shape factors. It is necessary to guess the shape of foundations and poor guess giving wrong estimation of bearing capacity.

In literature review, it has been discussed that Terzaghi (1943) was the first person to develop a comprehensive bearing capacity theory for shallow foundation. Based on the load failure mechanism shown in Fig 39, he developed equations of estimating bearing capacity of shallow foundations. The equation depends on the shape of foundations, which is shown in below

$$q_{ult} = 1.3c'N_c + qN_q + 0.4\text{YB}N_y$$

Where, N_c, N_q, N_y is dimensionless bearing capacity factor, c' is effective cohesion, q is surcharge at the ground surface.

In Ballina case, the undrained shear strength s_u at foundation level is given as 10 kPa, with 0° of friction angle and unit weight of sand 17 KN/m^2. By selecting Terzaghi's bearing capacity factor, the ultimate failure load is given as 332 KN, which is shown in Table 11.

Table 12.

Terzaghi's equation data

Terzaghi's bearing capacity factor			Effective stress/ Surcharge	Ultimate bearing capacity	Ultimate load failure
N_c	N_q	N_y	q = YD (KN)	q_{ult} (KPa)	Q (KN)

5.7	1	0	25.5	99.6	332

Original ϕ'(deg)	N_c	N_q	N_γ	Original ϕ'(deg)	N_c	N_q	N_γ
0	5.7	1.00	0	27	16.302	6.538	2.430
1	5.900	1.07	0.016	28	17.132	7.073	2.738
2	6.096	1.14	0.022	29	18.027	7.662	3.793
3	6.301	1.22	0.033	30	18.991	8.310	4.315
4	6.514	1.30	0.050	31	20.034	9.025	4.915
5	6.738	1.39	0.071	32	21.164	9.816	5.606
6	6.971	1.49	0.097	33	22.390	10.693	6.403
7	7.216	1.59	0.127	34	23.724	11.668	7.324
8	7.472	1.70	0.161	35	25.178	12.753	8.389
9	7.741	1.82	0.200	36	26.768	13.965	9.624
10	8.024	1.94	0.243	37	28.510	15.323	11.058
11	8.321	2.08	0.290	38	30.425	16.847	12.727
12	8.633	2.22	0.343	39	32.535	18.564	14.672
13	8.962	2.38	0.402	40	34.866	20.504	16.943
14	9.308	2.55	0.466	41	37.451	22.704	19.602
15	9.674	2.73	0.538	42	40.326	25.207	22.720
16	10.061	2.92	0.617	43	43.535	28.065	26.384
17	10.470	3.13	0.705	44	47.129	31.341	30.699
18	10.903	3.36	0.804	45	51.171	35.114	35.792
19	11.362	3.61	0.913	46	55.734	39.476	41.817
20	11.850	3.88	1.036	47	60.909	44.544	50.266
21	12.368	4.17	1.173	48	66.803	50.461	59.769
22	12.920	4.48	1.327	49	73.550	57.406	71.248
23	13.509	4.82	1.500	50	81.313	65.604	85.569
24	14.137	5.20	1.694	51	90.295	75.337	103.668
25	14.809	5.60	1.911	52	100.749	86.968	126.559
26	15.529	6.05	2.156	53	112.992	100.964	155.334

Figure 39. Terzaghi's bearing capacity factor (Geotechnical Engineering Design, 2015)

Skempton (1951) developed a simple equation to estimate the ultimate bearing capacity with factor N_c and undrained shear strength under undrained conditions. In literature review, it has been discussed that Susan, et al (2006) investigated the undrained bearing capacity of square footings and modified Skmpton's prediction of N_c to 5.9 for a rough square footing.

$$q_{ult} = c_u N_c$$

Table 13.

Terzaghi's equation data

Terzaghi's bearing capacity factor	Undrained cohesion	Ultimate bearing capacity	Ultimate load failure
N_c	c_u (KPa)	q_{ult} (KPa)	Q (KN)

5.9	10	59	191.2

In both equations, it can be found bearing capacity factors have a significantly influence to estimate the ultimate failure load. The empirical factors mainly depends on the internal friction angle, interaction between foundation and soil and shape of foundations. Many investigators modified bearing capacity factors in different methods and it is necessary to take all foundation design elements into account to get the reasonable results.

6 CONCLUSIONS

Bearing capacity plays an important role for foundation design and perhaps the most important part for soil engineering. Failing to recognise the bearing capacity can cause foundation failures and the entire building project becomes unsafe. In the past, the investigation of large-scale shallow foundation tests on soft clay is lmited. Most of data comes from UK's national soft soil test site, Bothkennar, Scotland. Australian National Field - Testing Facility was built in Ballina, NSW in 2013. The site investigation was conducted in this area and a series of in situ and laboratory tests were investigated.

The aim of this project was to investigate the bearing capacity behaviour of foundations especially for undrained bearing capacity of square footings on soft clays. With the literature review of fundamental knowledge of bearing capacity, it was found that Terzaghi's (1943) bearing capacity theory is most widely used one to estimate bearing capacity of shallow foundations. While Terzaghi's bearing capacity did not take the effects of footer depth, load inclination factor, soil compressibility, and water tables. Skempton (1951) reconsidered Terzaghi's equation and found bearing capacity factor N_c increase with foundation depth. The bearing capacity factor and shape factor he obtained was N_c = 6.17 and S_c = 1.2 for rough square footings. The other few studies such as Salgado (2004), Susan (2006) investigated the bearing capacity behaviour of square footings and proposed that N_c = 5.52, S_c = 1.1, N_c = 5.9, S_c = 1.15 respectively.

In Ballina case, the undrained shear strength relationship with its foundation relationship was investigated. The results obtained from modified Terzaghi's equation demonstrated that the undrained shear strength has a direct proportional relationship with ultimate bearing capacity. Q_u = 19.44 S_u. The results calculated from in situ tests- CPT and SBM indicate that both tests have reasonable estimation for ultimate bearing capacity within an error range of 5 %. While the laboratory tests- TC & TE can't predict the ultimate bearing capacity precisely. It has also been observed the TE test under estimate undrained shear strength around 20% and ultimate bearing capacity around 24%. For serviceability limit design, the effective settlements under working load is used to predict the foundation behavior. It was found that the secant shear modulus G_{10} and G_{MCCpm} can provide a good estimation of vertical settlement, while G_{MCCtx} also has a reasonable estimation.

In FEA analysis, a linear elastic Tresca soil model is adopted and applied using given data. The input data includes the previous test calculation such as undrained shear strength (10 kPa), Poisson's ratio (0.495), Young's modulus (3MPa), groundwater table (0.5m AHD), material unit weight etc. The load- settlement response of measured foundation performance from (UU) test was proved to be well predicted by numerical model. Through the output of deformation graph, it was observed that the gap between footing and excavation wall has a significant impact to the ultimate bearing capacity and vertical settlement. A non- liner curve demonstrated that the ultimate bearing capacity increase with decrease of gap between footing and slope.

9 REFERENCE

Abyaneh, SD, Ojo, A, Maconochie, A, Haghighi, A 2015, 'The undrained bearing capacity of shallow foundations subjected to three- dimensional loading Incuding Torison', *The twenty- fifth International Ocean and Polar Engineering*, pp 1-7.

Benmebarek, S, Saifi, I, Benmebarek, N 2017, 'Depth factors for undrained bearing capacity of circular footing by numercal approach', *Journal of rock mechanics and Geotechnical Engineering*, vol.9, pp 761-764.

Catanzariti, F 2016, 'Bearing capacity of shallow foundations', Geostru, p.11.

Du,p,Liu, XL & Zhang, YF 2017, ' Disscussion of the Method to Determine the Ultimate Bearing Capacity of Soil Foundation', *IOP Conference: Earth and Environmental Science*, pp 1-4.

Doherty, J.P, Gourvenec, S, Gaone, F.M 2017, 'Insights from a shallow foundation load-settlement prediction exercise', *Computers and Geotechnics*, Vol.93, pp 269-279.

Gui, D 1995, 'Bearing capacity of shallow foundation on simulated lunar soil', Master thesis, Montana State University, USA.

Gourvenec, S, Randolph, M& Kingsnorth, O 2006, 'Undrained bearing capacity of square and rectangular footings', *International Journal of Geotechnicals*, pp. 146-155.

Gagone, F.M, Gourvenec, S, Doherty, J.P 2018, 'Large- scale shallow foundation load tests on soft clay- At the National Filed Testing Facility (NFTF), Ballina, NSW, Australia', *Computers and Geotechnics*, Vol. 93, pp 253-268.

Hansen, J.B 1970,' A revised and extended formula for bearing capacity', Geoteknisk Institut, pp 4-10.

Hartsfiled, RJ 2013,' 'Upper bound analysis of bearing capacity and overturing capacities of shallow foundation in soft clay', Master thesis, Texas A&M University, USA.

Lianapathirana, D.S, Carter, J.P 2005, 'Undrained bearing capacity of Shallow foundations on structured soils', *Proceedings of the International Symposium on Frontiers in Offshore Geotechnics*, Western Sydney University, Sydney, pp 2-4.

Michalowski, R.I 2001, '*Upper-bound load estimates on square and rectangular footings*', Geotechnique 51, No.9, pp 787-798.

Mohamed, FMO 2014, ‘Bearing capacity and settlement behaviour of footings subjected to static and seismic loading conditions in unsaturated sandy soils’, Phd thesis, University of Ottawa, Canada.

Remai, Z 2012, ‘Correlation of undrained shear strength and CPT resistance’, Budapest University of Technology and Economics, pp 39-41.

Salagado, R, Lyamin, A.V, Sloan, S.W& Yu, H.S 2006, ‘Two and three- dimensional bearing capacity of foundations in clay’, Geotechnique 54, No.5, pp 297-306.

Sitharam, TG 2013,’ Advanced Foundation Engineering’, Shallow foundations, Indian Institute of Science, Bangalore.

Strahler, AW 2012, ‘Bearing Capacity of Immediate Settlement of Shallow Foundations on clay’, Master thesis, Oregon State University, USA.

Quadir, MA 1990, ‘Bearing Capacity of Strip Footing on Sand’, Master thesis, Bangladesh University, Dhaka.

Quoc, V.N 2008, ‘Numerical modelling of the undrained vertical bearing capacity of shallow foundations’, Master thesis, University of Southern Queensland, Queensland.

Xiao, M 2015, ‘*Geotechnical Engineering Design*’, The Pennsylavania State University, pp 10-16.